UNIVERSITY OF GHANA

SCHOOL OF ENGINEERING SCIENCES

SYNTHESIS AND CHARACTERIZATION OF ZINC OXIDE NANO-PARTICLES FOR PHOTOVOLTAIC APPLICATION

BY

GABRIEL KWAME SIPI TAKYI

(10373427)

A THESIS SUBMITTED TO THE SCHOOL OF GRADUATE STUDIES IN PARTIALFULFILMENT OF THE AWARD OF DEGREE OF MASTER OF PHILOSOPHY IN MATERIALS SCIENCE AND ENGINEERING

DEPARTMENT OF MATERIALS SCIENCE AND ENGINEERING

2018

DECLARATION

Candidate's Declaration

I hereby declare that this thesis which is the result of my own original research under strict supervision was prepared in accordance with the University of Ghana's academic regulations and that no part of this has been presented for another degree in this University or elsewhere.

Candidate's name: Gabriel Kwame Sipi Takyi

Signature: …… Date: ……..

Supervisors' Declaration

I hereby declare that the preparation and presentation of this thesis were supervised in accordance with the guidelines on supervision of thesis laid down by the University of Ghana.

Supervisor's name: Prof. Boateng Onwona-Agyeman, (University of Ghana)

Signature: …… Date: ……..

Co-Supervisor: Dr. Emmanuel Nyankson (University of Ghana)

Signature: …… Date: ……..

Head of Department's Declaration

I hereby declare that this thesis has been prepared, supervised and accepted in accordance with the guidelines on the thesis laid down by the University of Ghana.

Head of Department's name: Dr. Lucas Damoah

Signature: …… Date: ……..

AKNOWLEDGEMENT

My sincere appreciation goes to my supervisors Prof. Boateng Onwona-Agyeman and Dr. Emmanuel Nyankson. I also give appreciation to Dr. Benjamin Agyei-Tuffour, Dr. Lucas Damoah and all the lectures in the Materials Science and Engineering Department of the University of Ghana.

I owe a lot to Biotechnology laboratory centre and Ecological laboratory where I conducted my research. I also thank the laboratory technicians at the materials science department.

I also say thank you to all my mates.

DEDICATION

I dedicate this work to my lovely parents Mr. Kwamina Takyi and Ms. Sophia Essien, my uncle Mr. Timothy Kobina Essien and my lovely sister Christina Darko.

TABLE OF CONTENTS

LIST OF FIGURES

LIST OF TABLES

ABSTRACT

The low total conversion efficiency of dye sensitized solar cells have caused researchers to improve the individual components of the cell. This work aims to produce zinc oxide nanoparticles to help improve absorption and also reduce recombination in the photo anode of the dye-sensitized solar cell (DSSC). In this work, zinc oxide nanoparticles were produced using the hydrothermal synthesis technique and the annealing effect was conducted on the prepared samples.

The samples prepared were characterized using X-ray diffraction analysis (XRD), Scanning electron spectroscopy (SEM), energy dispersive spectroscopy (EDX), Fourier-transform infrared spectroscopy (FTIR), diffuse reflectance spectroscopy (DRS), thermal analysis (TGA/DSC).

The XRD results indicated that hexagonal wurtzite phase were produced with a dominate diffraction peak of (002) at the highest hydrothermal temperature and at the annealing temperature of 500 ℃ for 30 minutes.

The SEM results show nearly spherical particles with enhanced agglomeration whiles the EDX results confirmed the presence of zinc and oxygen elements without any impurity. The DRS results show a significant increase in absorption when the samples were annealed.

Furthermore, the TGA/DSC results showed the stability of zinc oxide above 400 ℃.

This study suggests that the synthesized zinc oxide nanoparticles might perform excellently in DSSC photo anode.

CHAPTER ONE

INTRODUCTION

Photovoltaics (PV) is the third renewable energy source after hydro and wind powers in terms of global capacity[1]. Semiconducting materials that exhibit the photovoltaic effect have received great attention in research over the years[2]. Examples of semiconducting materials for the photovoltaic applications are Silicon, CuIn(Ga)Se_2, CdTe, SnS TiO_2 and ZnO[3–5].

Irrespective of the source of light either natural (sunlight) or artificial, solar cells are described as being PV. Solar cells are generally classified into three (3) generations of cells. The first generation is based on silicon crystals such as monocrystalline silicon and polycrystalline silicone. The second generation of the solar cell are thin films. These cells are made from amorphous silicon, CIGS and CdTe. Dye Sensitized Solar Cells (DSSC) is the most common type of the third generation of the solar cells[6]. The low production cost and flexible production methods of DSSC has made it to gain great attention in research[1, 6–9].

Semiconductors with wide band gap are usually used as the photo-anode in DSSSC. The semiconductor helps in the efficient conversion of light into electrical energy [10]. The material for the photo-anode should have the property to reduce the electron recombination probability, fast charge transfer rate, large surface area and also improve the efficiency of the photo-generated electron transfer[10–12]. TiO_2 is one of the wide band gap semiconductors usually used as the DSSC photo anode[9, 10]. Although it has a large surface area, it also has weak electron mobility, slow transport and enhanced recombination of photo-excited electrons due to the numerous grain boundaries and disordered network. This makes researchers to find suitable alternative [10]. The similarities exhibited by the ZnO nano structures as compared to TiO_2 in terms of energy band structure and physical properties has made it an option to be used as photo-anode[13, 14].

Recently, the improved electron gathering, transport efficiency and reduced recombination exhibited by ZnO photo anode has made it a suitable alternative to replace the TiO_2 photo anode[15, 16].

ZnO, a II-VI metal-oxide semiconductor is an example of a wide band gap semiconductor which exhibit quantum confinement effect in an experimentally accessible size range[15, 16]. At room temperature, the band gap of ZnO is 3.37 eV and an excitation binding energy of 60 meV [16–20]. ZnO is abundantly available and very economical. It has excellent chemical and thermal stability, low cost, biocompatible and environmentally friendly. Due to these interesting properties, ZnO has variety of applications in photonics, transparent electrodes in solar cells, spintronics, transparent UV- protection films, varistors, transducers and piezoelectric applications[17, 18, 21, [22].

ZnO nano powders can be prepared by several well-established physical and chemical synthesis techniques. Mainly, it is prepared from solution based precursors. Literature has reported many methods such as mechanochemical-thermal synthesis[25], spray pyrolysis[26], laser ablation[27], electrochemical depositions, sol-gel method, microwave synthesis, chemical-precipitation method, hydrothermal method and so on[16, 18, 23–26]. However, most of these synthesis routes requires high temperature processing which usually leads to the evaporation of some volatile species in the sample[19, 27].

The hydrothermal method is one chemical synthesis technique which is promising. This method progresses in a closed system with high autogenous pressure. Variations in the source species (concentrations of reactants), reaction time and temperature controls the particle properties such as morphology and size of the prepared material[17, 18, 21].

The annealing and the conditions at which ZnO is prepared has a great influence on the defects in the ZnO NPs.

The effect of annealing conditions on defect-related emissions on thin-films and nanostructured ZnO have been conducted [28–30]. The annealing removes internal tension in the ZnO and enhance electrical and optical properties of the material[28, 31, 32].

The common types of annealing are vacuum-annealed and air-annealed.

Research shows that, the low dark current of the air-annealed ZnO makes it a suitable candidate for photodetector applications[36].

Varying annealing temperatures in oxygen can control ZnO prepared at low temperatures[6].

A lot of studies have been done on the effect of preparation conditions and the annealing temperatures of ZnO prepared by sol-gel and modified sol-gel techniques.

It is however important to study the effect of annealing and the different hydrothermal temperatures for preparing ZnO using the hydrothermal methods.

In this work, a chemical synthesis of ZnO is produced using the hydrothermal synthesis technique. Two different categories of samples are prepared denoted as as-prepared and annealed samples. The as prepared are samples without any annealing and the annealed are the samples which has been treated after the preparation. The effect of the annealing and the preparation conditions of the synthesised samples prepared using the hydrothermal technique will be compared.

The samples produced will be characterized using XRD, SEM, EDX, DRS, FTIR and TGA.

Problem Statement

The challenge of poor electron gathering, transporting efficiency and inhibiting charge of TiO_2 has caused researchers to find alternative wide band gap semi-conductor materials for the DSSC photo anode[11, 14, 34].

The two key characteristic properties of photo anode materials are large surface area necessary to ensure high dye loading and fast charge transport rate to ensure high electron collection efficiency[11].

The improved electron gathering, transport efficiency and reduced recombination exhibited by ZnO photo anode has made it a suitable alternative to replace the TiO_2 photo anode[15, 16].

The nanostructured ZnO is ideal since it possesses large surface area as compared to the bulk materials which do not allow high dye loading.

Aim and objectives.

The aim of this research is to synthesize ZnO nanoparticles, assess the effect of annealing on its properties and its potential application in photovoltaics.

The objectives of this work are as follows.

- Synthesize ZnO nano particles from solution based precursors using the hydrothermal technique.
- Asses the effect of the processing conditions and the annealing on the properties of the prepared material.

- Characterize the samples produced using XRD, SEM, EDX, DRS, FTIR, TGA and compare their properties.
- Assess the potential of ZnO material to be used as a photovoltaic application.

Scope of Study

This project will help in the effective conversion of sunlight into electricity in one of the components of the photovoltaic devices by helping reduce recombination and slow transport of photo-excited electrons.

Structure of thesis

This report consists of five chapters. The first chapter is the introduction, the second is the literature review, the third chapter is the experimental methods, the fourth chapter is the results and discussion, the fifth chapter is the conclusion and recommendations and the references.

CHAPTER TWO

LITERRATURE REVIEW

2.1 Background

This chapter reviews relevant literature related to the work.

Nanomaterials

Nanomaterials have gained attention in research because of their distinguished performance in electronics, photonics and optics[38]. With nanomaterials, researchers realized the importance of the effect particle size has on the physical and chemical properties of materials[39]. Materials in the nanometre range have size dimensions between one nanometre (1 nm) to one hundred nanometres (100 nm). The shape of nanomaterials can be one dimensional (1 D), two dimensional (2 D) and three dimensional (3 D)[40].

Nanoparticles are classified based on the morphology, size, physical and chemical properties. Some of the well-known NPs based on the physical and chemical properties are carbon based NPs, metal NPs, ceramic NPs, polymeric NPs and semiconductor nanoparticles.

Nanostructured materials have high surface to volume ratio, high aspect ratio, the conduction of materials become insulators below a critical length scale as energy bands ceases to overlap and the conduction in highly confined structures such as quantum dots is very sensitive to the presence of other charged carriers and hence the charge state of the dot[41].

These properties of nanomaterials have made them very useful in photo anode applications. Zinc oxide, titanium dioxide, etc. are examples of semiconductor nanomaterials that are usually used in photo anode applications.

The large surface area and fast charge transport rate exhibited by ZnO makes it a better choice for the photo anode application.

Zinc Oxide

The use of zinc compounds either in processed or unprocessed form can be dated back as far as 500 BC. These zinc compounds were usually used as paints, medical ointment, etc. but no knowledge of their composition was not known.

A Greek physician Dioscorides mentioned of the use of zinc oxide as an ointment in the 1st century AD. Around 1025 AD, ZnO was used to treat skin conditions including skin cancer.

In 1850, the use of zinc oxide also known as zinc white because of it colour became very popular.

Since the 1960s, ZnO thin film synthesis has been an active area due to their interesting properties and applications. Researchers have developed a lot of processing methods. It was found that varying the processing parameters like precursor concentration, time, temperature and the post treatment (air-drying, annealing and calcination) of the materials give varying properties and structure for different applications[36–41].

ZnO has captured a lot of attention in research due to the fact it is a wide band gap semiconductor

2.2 Structures of ZnO

2.2.1 Crystal structure

ZnO has three crystal structures. They are the hexagonal wurtzite, cubic zinc blende and cubic rock salt crystal structures. The hexagonal wurtzite structure and the cubic zinc blende are the common ones' whiles the rock salt is rarely found[24,39, 42–[45].

Electrical neutrality is maintained in most materials because of the reconstruction of the planes at the atomic level but ZnO is an exception [43]. This is due to the fact that the

surfaces are flat, stable and exhibit no reconstruction resulting from the zinc and oxygen planes being electrically charged because of the polar Zn-O bonds[49].

Hexagonal wurtzite structure

The hexagonal wurtzite structure is the thermodynamically stable phase of ZnO[45–47]. This makes zinc blende to slowly transform into wurtzite[53]. This behaviour is characterised by the property that an increase in temperature decreases density. Cubic closest packing structures (ccp) are denser than hexagonal closest packing structures and this also favours the conversion of the zinc blende (sphalerite) to wurtzite over time[50]–[52], [54], [55]. Another factor that causes the tendency to form the wurtzite rather than the zinc blende is the large ionic bonding (Zn^{2+} - O^{2-}) in the ZnO bond corresponding to the radius 0.074 nm for Zn^{2+} and 0.14 nm for O^{2-} [18], [50].

The wurtzite has a hexagonal closest parking structure (hcp)[50]. This is characterised by 12 ions in the corners of each unit that create a hexagonal prism. The lattice parameters of the wurtzite are a = 0.3296 mm and c = 0.52065 nm. The deviation of the wurtzite structure of the ZnO from the ideal wurtzite structure changes the c/a ratio to approximately 1.60 as compared to the ideal value 1.633. Lattice instability and iconicity of the ZnO structure are probably the cause of the deviation of the ZnO wurtzite from the ideal wurtzite structure [55][56][50]. The space group of the hexagonal structure is $P6_3mc$ (C^4_{6v}) and a point group pf 6 mm in Herman-Mauguin notation or C_{6v} in the Schoenflies notation [50].

Cubic Zinc Blende Structure

The cubic Zinc blende structure is also called sphalerite. This is characterised by the cubic closet packing (ccp) which is also known as face-centred cubic.

The zinc blende ZnO structure is not a thermodynamically stable structure The zinc blende structure has the space group F43m in the Hermann-Mauguin notation and T^2_d in the Schoenflies notation[50].

The only difference in the wurtzite and zinc blende structure is the bond angle of the second-nearest neighbours[50], [56].

The rocksalt structure of the ZnO

The rocksalt structure is only observed at relatively high hydrostatic pressures above 10 GPa. The reduction in the lattice dimensions causing the interionic Coulomb interaction to favour the iconicity more over the covalent nature is the reason causing this observation[50], [55].

It has a space group structure of Fm3m in the Hermann-Mauguin notation and O5h in the Schoenflies notation[50].

The rocksalt structure has a six-fold coordination and cannot be stabilized by the epitaxial growth as in the zinc blende[50].

Figure 2.1 show the three crystal structures of Zinc oxide.

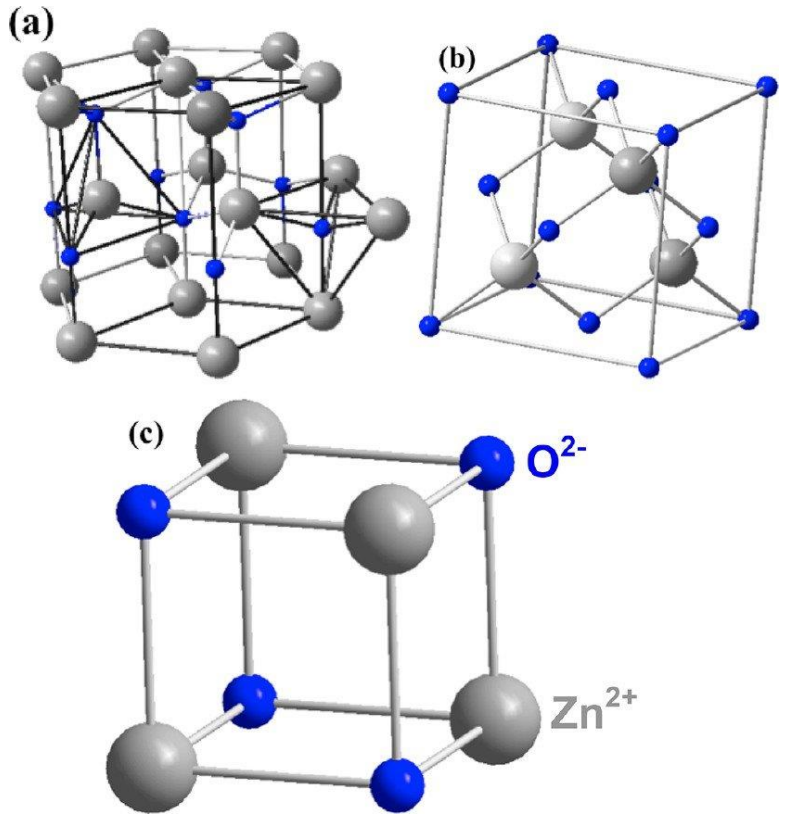

Figure 2.1:Crystal structure of ZnO. (a) hexagonal wurtzite; (b) cubic zinc blende ; (c) rock salt.[57]

2.2.2 Surface structure

Surfaces are also another important characteristic of every material. There are three surfaces and directions which are of special importance. They are (0001), $(11\bar{2}0)$ and $(1\bar{1}00)$ planes and their respective directions are $< 0001 >$,$< 11\bar{2}0 >$ and $< 1\bar{1}00 >$[50], [56], [58]–[63].

ZnO possess both polar surface and non-polar surface. The basal plane is the most common polar surface. The polar surfaces of most materials exhibit massive surface reconstructions to maintain stable structure but ZnO $\pm(0001)$ is an exception[62].

The other two which are commonly observed surfaces for ZnO are $\{2\bar{1}\bar{1}0\}$ and $\{01\bar{1}0\}$. The $\{0001\}$ surfaces has a higher energy as compared to the non-polar surfaces [60]–[63].

2.2.3 Growth structure

ZnO exhibit three fast growth directions from crystal structure. They are <0001>, <01$\bar{1}$0> and <2$\bar{1}\bar{1}$0> combined with the (0001) polar surfaces. Different growth structures can be developed by varying the growth rate along these directions owing to the atomic terminations of the polar surfaces. Under given conditions, factors that determines the morphology of a material includes the relative surface activities of the numerous growth facets. A controlled condition depends on the different kinetic parameters for different crystal planes. A crystal usually develops into a three-dimensional object with well-defined and crystallographic faces with low energy.

2.3 ZnO Nanoparticles: Properties and their potential applications

ZnO nanoparticles is useful in wide range of applications due to its unique and interesting physical and chemical properties. These properties make ZnO a suitable candidate in a wide range of applications ranging from electronics, spintronics, optoelectronics, piezoelectricity, Li-ion batteries, rubber industry, ceramic industry, medicine to mention a few.

The direct wide band gap of the ZnO has made it to gain attention in research of late.

Examples of properties unique to ZnO are the direct and wide band gape, large exciton binding energy, strong photoluminescence, high thermal conductivity, radiation hardness, strong non-linear resistance of polycrystalline ZnO, large piezoelectric constants, large non-linear optical coefficients, etc.

Here, a few of the properties are selected and their usefulness in applications are discussed.

Direct and wide band gap

Wide band gap refers to materials that have their band gap to be in the range of 2-4 eV. These materials have their electronic properties falling between semiconductors and insulators[30], [47], [53], [64]–[66].

ZnO has a room temperature band gap of 3.37 eV and 3.44 eV at low temperatures. A semiconductor with a large band gap has key advantages which include the ability to sustain large electric fields, higher breakdown voltages, lower electronic noise, high temperature and high power operation. The wider band gap allows wide band gap devices to operate at much higher temperatures on the order of 300 ^{o}C[1].

In optical properties, the wavelength at which LEDs can emit and the wavelength at which photovoltaics operate most efficiently are all determined by the band gap[67].

“Alloying ZnO with MgO can modify the band gap from 3-4 eV. The conductivity of ZnO is always n-type when prepared. Doping p-type ZnO has proved unsuccessful over some time [22], [43], [59]. Researchers attribute the reason that ZnO has the tendency toward n-type. The very few candidate shallow acceptors in ZnO is also a reason for the ZnO tendency to form n-type conductivity[68]–[71].

These qualities of the direct and wide band gap of the ZnO makes it fascinating in band gap base devices like photovoltaics, optoelectronics, LEDs, laser diodes, etc “ [24][72].

Binding energy

ZnO has a large exciton binding energy of 60 meV as compared to other semiconductors like GaN which has an exciton energy of 25 meV which is also considered as a large exciton energy[12], [20], [43].

Exciton is a bound state of an electron and a hole. The absorption of photons by a semiconductor forms an exciton. This is one of the key importance for the optical properties of a material. The exciton binding energy gives the stability against thermal dissociation of excitons. The large exciton energy of the ZnO also results in bright room temperature emission[22].

These qualities of the large exciton energy of the ZnO makes it the best option for room temperature operation of any application which is exciton-based. Lasers, optical fibre, etc. are examples of optical devices which are exciton based[73]–[75].

Strong luminescence

ZnO exhibit two luminescence bands by all the various forms. A short wavelength band and a broad wavelength band. The short wavelength is located near the absorption edge of the crystal whiles the broad wavelength band is the maximum which is usually in the green spectral range[24], [59], [72].

The strong luminescence of ZnO makes it a suitable candidate in phosphor applications[72].

As at now, research is still on-going to better understand the source of the luminescence centre and the luminescence mechanism which is commonly ascribed to oxygen vacancies or zinc interstitials with no base fact[43], [59]. Research shows that, these oxygen vacancies or zinc interstitial defects cannot emit in the green region. Other researchers are suggesting that zinc vacancies are probably the reason for the green luminescence. As mentioned earlier, the zinc vacancies are also one of the reasons that gives preferential formation of ZnO n-type conductivity[43][76][77].

Piezoelectric constants

Piezoelectricity is due to atomic scale polarization. The piezoelectric effect can convert a mechanical vibration into an electric signal or vice versa[28][47].

Crystals are deformed and vice-versa when voltage is applied to piezoelectric materials. The strong piezoelectric and pyroelectric properties arise because of the low symmetry in the wurtzite crystal structure and large electromechanical coupling. [34], [49], [60], [78]. These materials taking advantage of the properties makes them preferred in applications like sensors, actuators and transducers.

High thermal conductivity

ZnO is applied in the rubber industry as additives in order to build-up the thermal conductivity of tires due to the high thermal conductivity of the ZnO. High efficiency of heat removal during device applications is also one of the advantages of the high thermal conductivity property[11, 18]

Large crystals

One of the key advantages in semiconducting materials is the availability of large crystals for device applications.

The large single crystals available in ZnO over its counterpart GaN makes it possible to produce quality thin films with reduced concentrations of extended defects[43].

Radiation hardness

Materials for high altitude applications requires the property of radiation hardness. ZnO exhibit excellent radiation hardness better than GaN [36].

Amenability to wet chemical etching.

Low temperature chemical etching is one of the benefit of semiconductor materials for device fabrication. The amphoteric nature of ZnO make it possible for ZnO thin films to be etched with both acids and alkaline solutions.

The low-temperature chemical etching add great flexibility in the processing makes it a good candidate for electronic and optoelectronic devices[65].

2.4 Synthesis and Growth of ZnO

Generally, the properties and structure of any material greatly depends on the preparation method used.

Due to the great influence of particle size on the physical, chemical and structural properties of materials, researchers have developed various methods to produce materials in the nanometre scale.

From literature, researchers have been successful in developing most of the materials in the nanometre scale. Semiconductor materials are one of the areas in which their materials can be synthesized in the nanometre range. Examples of semiconductor materials that can be synthesized in the nanometre scale are titanium dioxide, zinc oxide, copper oxide to mention a few.

Various methods have been used to synthesis ZnO nanoparticles. These methods are broadly divided into two main classes. They are bottom-up approach and top-down approach. The

operations, reaction conditions and adopted protocols further divides the two main synthesis classes into sub-classes.

Figure 2.2 is a shematic diagram showing the typical synthetic methods for producing nanoparticles.

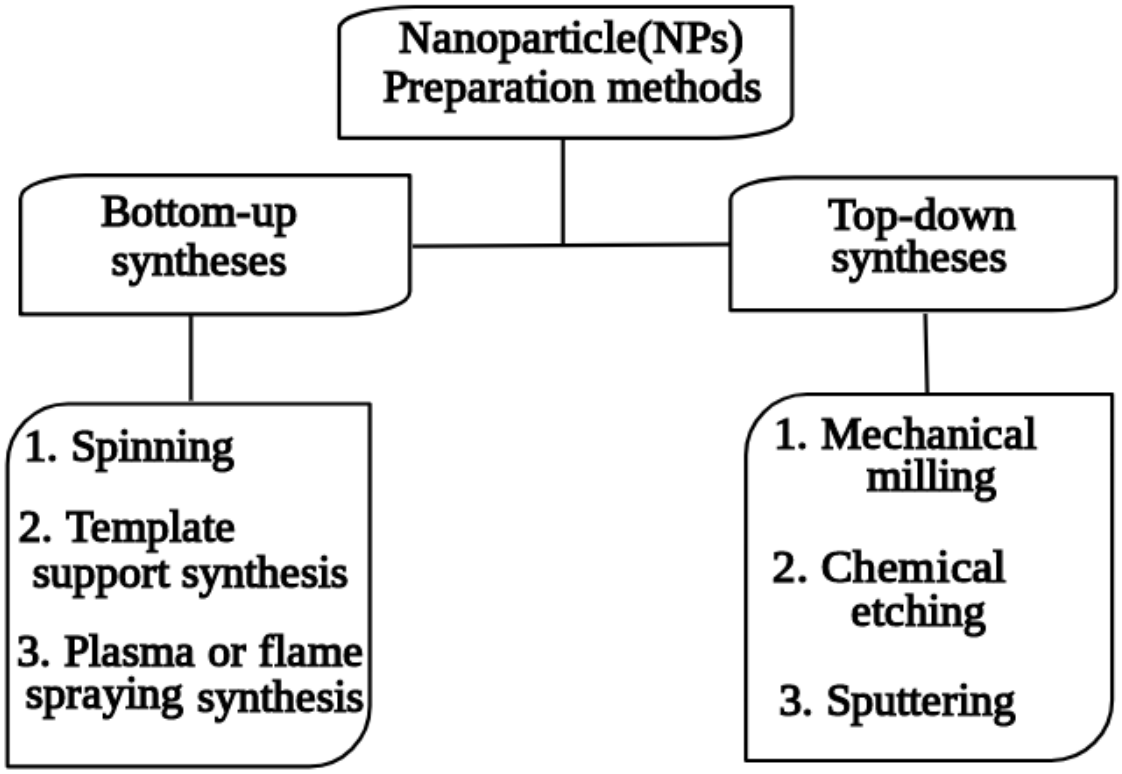

Figure 2.2: The two main classes of nanoparticle synthesis and some sub-classes.

2.4.1 Top-down approach

This approach involves the reduction of a larger molecule into smaller molecules in the nanometre scale. Mechanical milling, chemical etching, sputtering, laser ablation and electro-explosion are some examples of the top-down approaches for synthesising nanomaterials.

Although literature reports the synthesis of nano-size coconut shells by employing the milling method and the synthesis of spherical magnetite nanoparticles from natural iron oxide

(Fe_2O_3), this route by nature is not cheap, quick to manufacture and not suitable for large scale production[39], [81].

2.4.2 Bottom-up approach

This approach is the reverse of the top-down method. Here, nanoparticles are formed from relatively simpler substances by building up atoms or molecules up to nanostructures.

Examples of this approach are sol gel, green synthesis, spinning, hydrothermal and biochemical synthesis.

The advantages of this approach being cheap, quick to manufacture and industrial large scale production as compared to the top-down approach makes it suitable for producing most of the materials in the nanometre scale[39].

In this approach, most of the nanomaterials are prepared using solution based precursors. ZnO and TiO_2 nanoparticles have been produced using the sol gel method in this approach.

2.4.3 Zinc oxide nanoparticle synthesis.

Both the top-down and the bottom-up approach have been used to synthesise ZnO nanoparticles. The bottom-up approach is the most widely used because of the advantages mentioned earlier.

In this sub-section, a partial list of some of the synthesis techniques is discussed.

2.4.3.1 Sol gel method

The sol-gel method has gained a lot of attention due to the low cost, reliability, reproducibility and moderately mild synthesis conditions[84–86]. The variations of properties of this method extends its range of applications.

This method of processing nanostructures begins with Nano size unit and it also undergoes reactions on the nanometre scale hence resulting in the formation on materials in the nano meter scale. The sol-gel method has gained great attention by researchers because of the purity of the starting materials as well lower processing temperatures. Also, by adopting this method, the powder size, morphology and surface chemistry are controlled simultaneously[24], [45], [85].

2.4.3.2 Hydrothermal / Solvothermal technique

The hydrothermal or solvothermal is a technique that has received great attention in research owing to the advantages in the processing of nanostructured materials for a wide variety of technological applications[20].

The hydrothermal process is a chemical reaction which occurs in the presence of aqueous solvents or mineralizers under specific temperature and pressure. Solvothermal is the same concept as hydrothermal just that the reaction takes place in the presence of non-aqueous solvents[86], [87].

This method progresses in a Teflon lined autoclave at specific temperatures and pressures. The mixture of substrates in the autoclave is gradually heated to the required temperature and pressure and then left for it to cool slowly. The heating followed by cooling results in the formation of the nuclei and subsequently nuclei growth[24].

This method is very simple and environmentally friendly due to the fact that it does not require further processing.

The high degree of crystallinity, high purity of the material obtained, low process temperature and pressure are some of the advantages of the hydrothermal method[23], [88]–[93].

CHAPTER THREE

EXPERIMENTAL METHODS

3.1 Materials

The chemical used in this work were of analytical grade and were used as purchased. The reagents used in this work were zinc acetate dehydrate, sodium hydroxide and methanol were all purchased from Sigma Aldrich.

3.2 ZnO nanoparticle synthesis

The hydrothermal process was used for the synthesis of the nanostructured zinc oxide. The equipment used for the hydrothermal synthesis is the Teflon-lined stainless steel autoclave.

3.2.1 Hydrothermal technique

The hydrothermal synthesis of the ZnO is demonstrated in the Figure 3.1.

Zinc acetate and methanol were used as precursors. A zinc acetate solution of 0.5 M was prepared in 50 ml of methanol under stirring. To this solution, 25 ml of 1 M NaOH was added drop-wise under continuous stirring at room temperature forming transparent white solution which then turns milky. The pH of the solution was adjusted to 8 using NaOH. Teflon-lined stainless steel autoclave was used for the hydrothermal treatment by varying the temperatures (90, 100, 110 and 120 ℃) for 6 hours at a pressure of 4 bar.

The solution was left to cool naturally to room temperature. Methanol was used to wash the resulting product , filtered and then dried in a laboratory oven at 60 ℃. Part of each of the prepared samples were annealed in a Thermolyne oven at 500 ℃ for 30 minutes.

The flow diagram and the images for the entire synthesis method is presented in Figures 3.1 and 3.2, respectively. The formation of the ZnO nanoparticles from this synthesis method can be described by the reactions below:

$$Zn(CH_3COO)_2.2H_2O + 2NaOH \longrightarrow Zn(OH)_2 + 2CH_3COONa + 2H_2O \quad (3.1)$$

$$Zn(OH)_2(gel) + 2H_2O = Zn^{2+} + 2OH^- + 2H_2O = [Zn(OH)_4]^2 \quad (3.2)$$

$$[Zn(OH)_4]^{2-} \rightarrow ZnO_2^{-2} + 2H_2O \quad (3.3)$$

$$ZnO_2^{-2} + 2H_2O \rightarrow ZnO + 2OH^- \quad (3.4)$$

The growth mechanism of the zinc oxide nanostructure is an intricate process. This is usually studied to compose of two main steps: the generation of the nuclei and the subsequent crystal growth of the nuclei forming the zinc oxide. The $Zn(OH)_4^{2-}$ complexes serve as basic growth units for the preparation of zinc oxide nanostructures[94].. When the concentration of Zn^{2+} and $OH-$ reaches super saturation degree ,ZnO nuclei will form according to the reaction (3.4) .

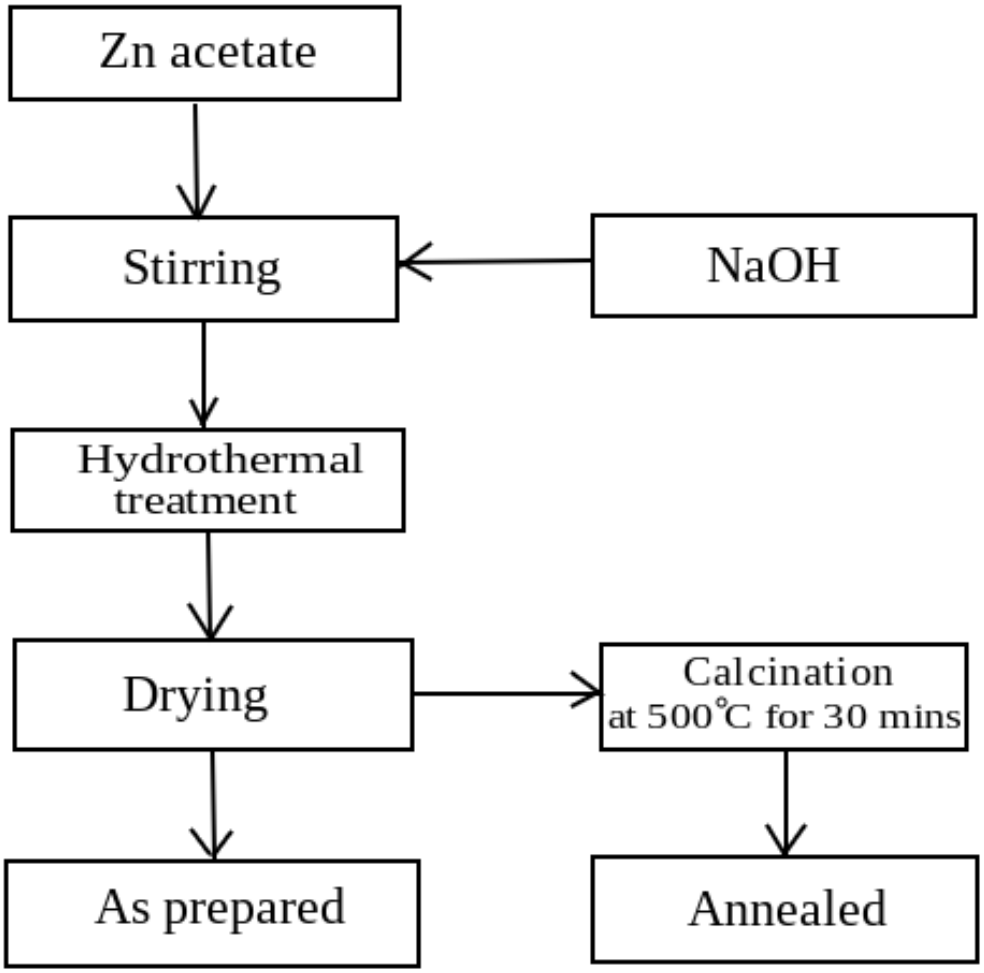

Figure 3.1: Flow diagram of the synthesis of ZnO nanoparticles via the hydrothermal method.

Figure 3.2: Flow chart highlighting the stages of the synthesis process.

3.3 Characterizations

3.3.1 X-ray Diffraction Spectroscopy (XRD)

XRD technique was used to analyse the phases present and the crystalline nature of the synthesized zinc oxide nanoparticles. The XRD patterns were obtained using Bruker D8 theta with anode material = Cu K-Alpha1 [Å]: (1.54060) and generator settings (40 mA, 45 kV). Derby-Scherer's equation was then used to calculate the average crystallite sizes of the synthesized ZnO from the obtained XRD patterns.

3.3.2: Fourier Transform Infra-Red Analysis (FTIR)

The functional groups of the synthesized ZnO nanoparticles were characterized by the Fourier transform infrared (FTIR) spectroscopy in the range $4{,}000\,cm^{-1} - 500\,cm^{-1}$

3.3.3 Scanning Electron Microscope (SEM) and Energy Dispersive Spectroscopy (EDX)

The morphology and elemental information of the samples were examined by using FEI Nova NanoSEM 450 fitted with EDX acquisition detector

3.3.4 Diffuse Reflectance Spectroscopy (DRS)

Ocean optics USB-400 spectrometer with a dedicated reflectance probe was used to analyse the optical properties of the prepared samples. Illumination was supplied by a Halogen/Deuterium source across the UV-Vis range.

This technique was used to analyse the optical properties of the synthesized ZnO nanostructures. The Kubelka-Munk's function was used to calculate the band gap of the samples

3.3.5 Thermogravimetric Analysis (TGA) and Differential Scanning Calorimetry (DSC)

The thermal properties of the samples were determined using differential scanning calorimetry and thermal gravimetry analysis (DSC/TG) using NETZSCH STA 409 EP instrument.

22.3 mg of the sample was heated in synthetic air in an Al_2O_3 crucible up to 800 ℃ at a heating rate of 10 K/min.

CHAPTER FOUR

RESULTS AND DISCUSSION

4.1 Sample Identification

The two categories of the samples are named according to the hydrothermal temperature used for the preparation and the annealing temperature. The samples with A preceding their names denote the As-prepared samples without annealing whiles the ones with C denotes the As-prepared samples which have been annealed in air at 500 ℃ for 30 minutes.

- The As-prepared samples are A90, A100, A110 and A120.
- The annealed samples are C90, C100, C110 and C120

4.2 X-Ray diffraction spectroscopy analysis (XRD)

The XRD patterns obtained for the as-prepared and annealed samples are shown in Figure 4.1 and Figure 4.2, respectively. The XRD peaks confirmed the formation of zinc oxide and the crystallinity increased with increasing hydrothermal temperature and at the annealing temperature. In conformity with the aforementioned processes, zinc oxide Nano powders were produced. The characteristic diffraction peaks at 2θ values 31.78°, 34.39°, 47.60°, 56.61°, 62.87°, 66.98° corresponds to the (100), (002), (101), (102), (110), (103) and (112) crystallographic planes, respectively. There were no other phases were present which suggested the high purity of the prepared sample from the annealing process. These characteristic diffraction peaks of the samples indicate the hexagonal wurtzite structure bears the same characteristics as shown by the diffraction peaks of the sample (Figure 4.1 and 4.2) [24], [85], [95]. The crystalline diffraction data shown can be confirmed with (JCPDS 36-1451)[7], [64], [83].

Although zinc oxide powders were directly synthesized during the hydrothermal process, it was observed that at lower hydrothermal temperatures the peaks were not distinct in the as-prepared samples and shown more of amorphous nature. The peaks become more distinct and sharper with increasing hydrothermal temperatures as well as at an annealing temperature of 500 ℃. This is due to the fact that the nucleation and growth of zinc oxide crystals is dependent on the hydrothermal conditions as well as annealing temperatures.

In Figure 4.2, it was observed that, the sample synthesized hydrothermally at 120 ℃ and at the annealing temperature of 500 ℃ for 30 minutes shows high degree preferential orientation of the (002) diffraction peak whiles the other samples show preferential orientation of the (001) diffraction peak. The most dominant peak at 34.39° corresponding to zinc oxide plane (002) (JCPDS 36-1451) indicate that the nanoparticles preferentially grow along the c-axis crystal plane of the ZnO Wurtzite structure when zinc oxide is prepared at hydrothermal temperature of 120 C followed by annealing in air at 500 °C for 30 minutes. The high intensity of the (002) diffraction peak is very crucial and significant for optoelectronic applications especially solar cells and LEDs.

The crystallite sizes of the samples were calculated by the Derby-Scherer equation (Equation 4.1) and the data were listed in Table 4.1

$$d = \frac{\kappa\lambda}{\beta\cos\theta} \qquad (4.1)$$

Where d, λ, κ , β and θ are the crystal size , X-ray wavelength (0.154 nm), Scherer constant (0.89), the peak full width at half maximum (FWHM) and the Bragg diffraction angle, respectively.

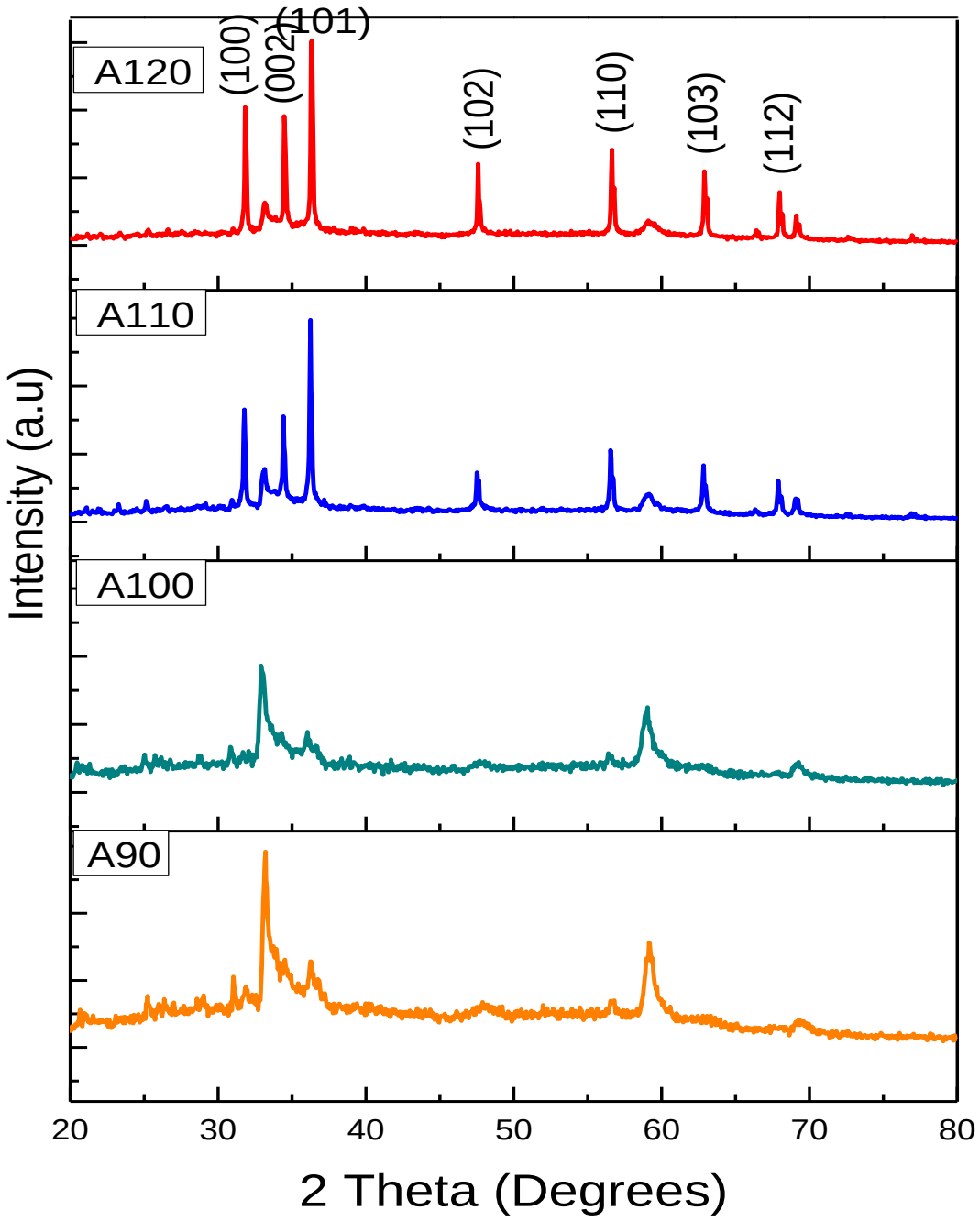

Figure 4.1: XRD Patterns of As-Prepared Samples varying hydrothermal temperatures.

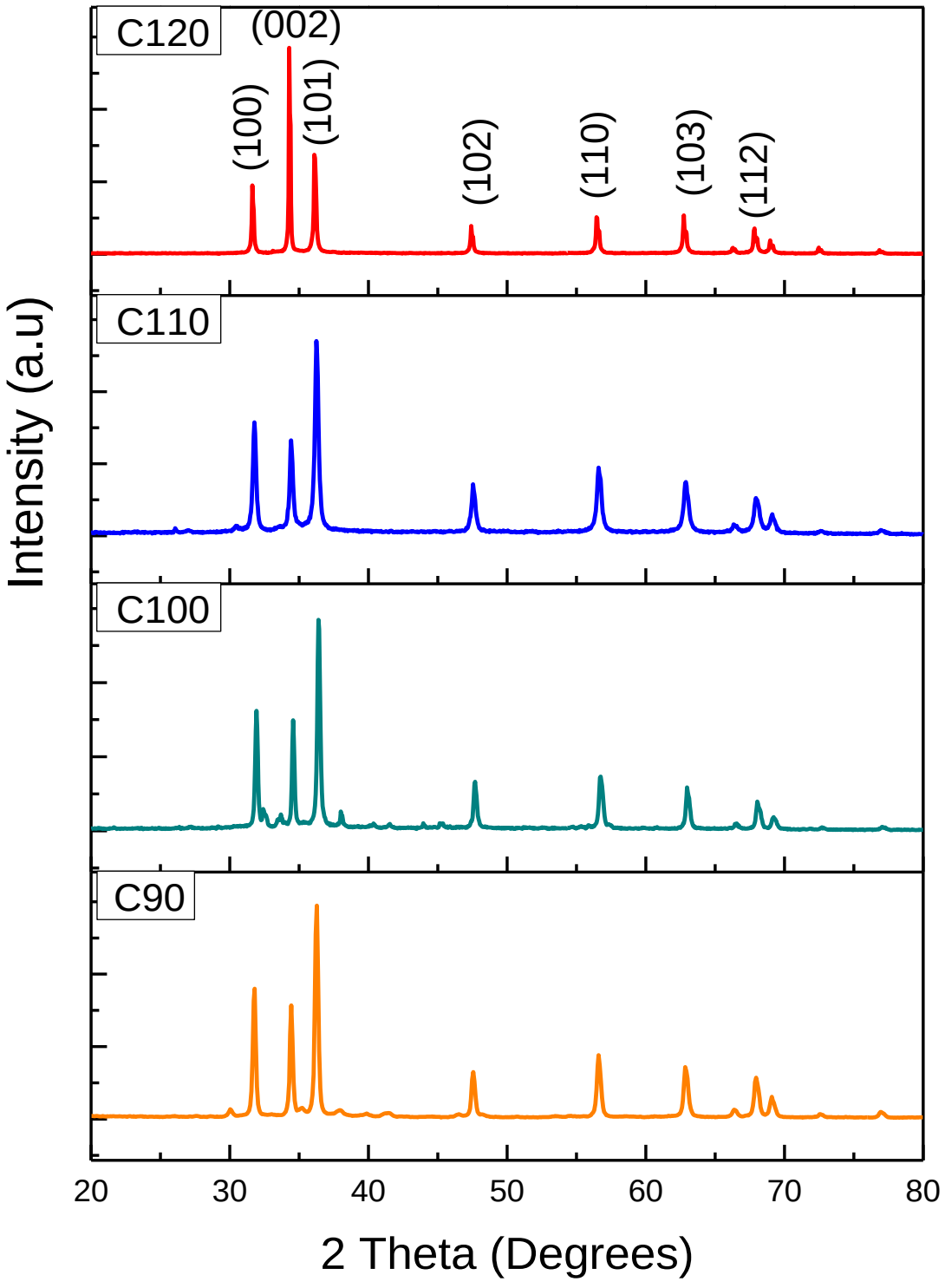

Figure 4.2: XRD Patterns of annealed Samples varying hydrothermal temperatures

Table 4.1: Average crystallite size and other parameters derived from XRD data.

Sample	Peak position 2θ (°)	FWHM 2θ (°)	Crystallite size (nm)
A90	34.04	5.03	1.73
A110	34.56	5.64	1.54
A120	34.82	5.37	1.62
C90	36.26	0.28	31.13
C100	36.41	0.25	33.90
C110	36.27	0.33	25.77
C120	34.31	0.16	54.64

4.3: Fourier Transform Infra-Red Analysis (FTIR)

The FTIR analysis was conducted on the samples to identify the organic and inorganic functional groups present in the samples prepared. The bombarded high energy spectrum causes the bending and stretching within the material.

Figure 4.3 and Figure 4.4 shows the FTIR analysis of the as-prepared and annealed samples, respectively. The peak corresponding to the Zn-O bond vibration at 531 cm^{-1} wave number is observed. The broad peak at 3438 cm^{-1} can be attributed to the presence of symmetric vibrations of –OH (hydroxyl groups) and C=O[17], [83]. This is due to the atmospheric moisture and molecules of CO_2, respectively. The C=O peak could have also resulted from the zinc acetate precursor used in the synthesis. The absorption bands at 1050-1650 cm^{-1} implies the presence of stretching vibrations of the CO-Zn and the –OH group on the surface

of ZnO nanoparticles. This result is similar to those reported in literature [32-37]. It can be noted that the FTIR results of the as-prepared and annealed samples are similar. In addition, the XRD confirmed the formation of ZnO for both the as prepared and annealed samples implying that hydrothermally prepared samples need not to be annealed in order to form ZnO.

It can also be observed in Figure 4.4 that annealing the samples with the increasing hydrothermal temperatures removes all the organic compounds and the molecules of water present. This can also be confirmed by XRD as the samples become more crystalline with sharper peaks. The results from the XRD and FTIR confirmed the synthesis of high purity ZnO nanoparticles.

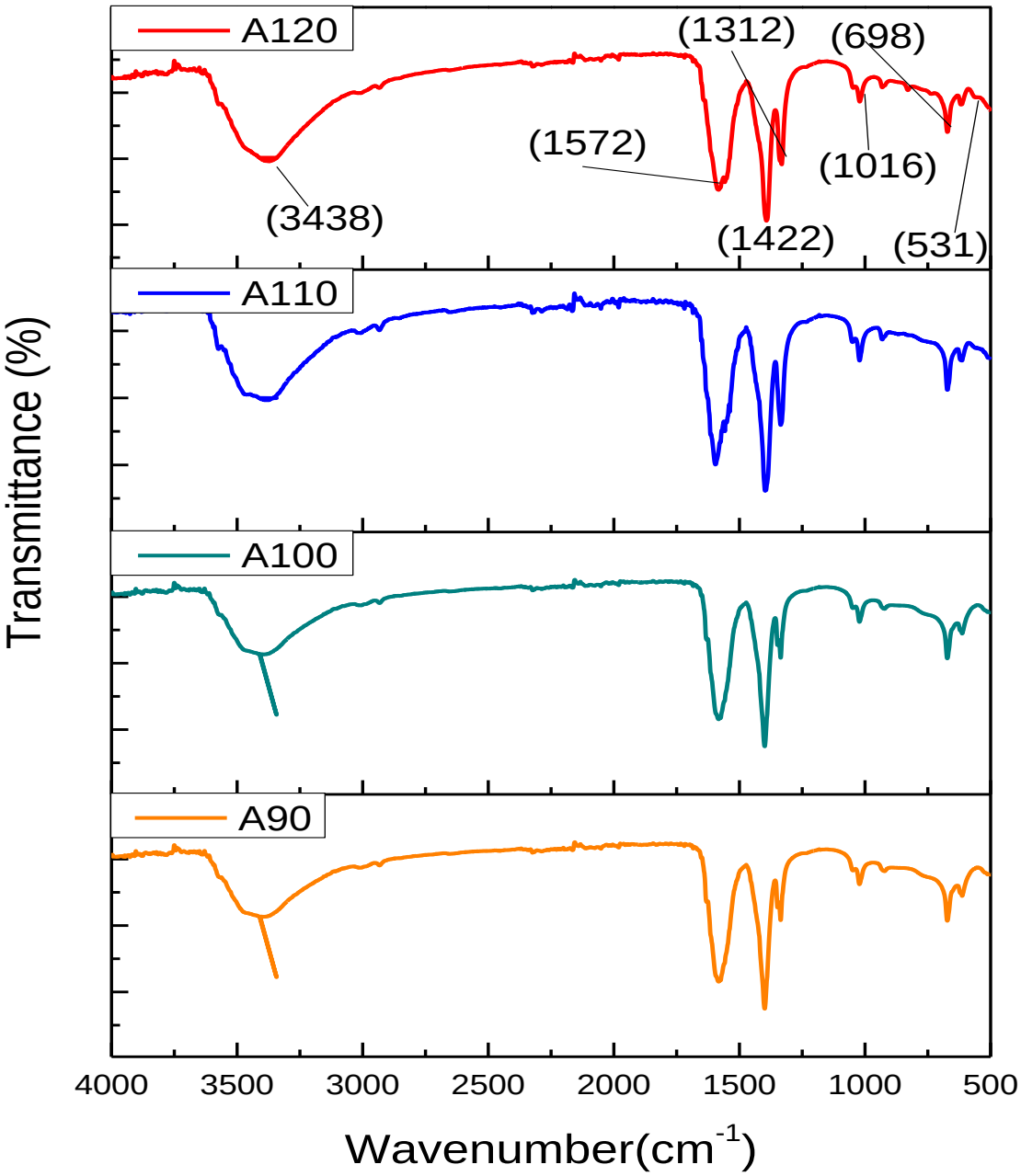

Figure 4.3: FTIR spectra of As-Prepared Samples varying hydrothermal temperatures

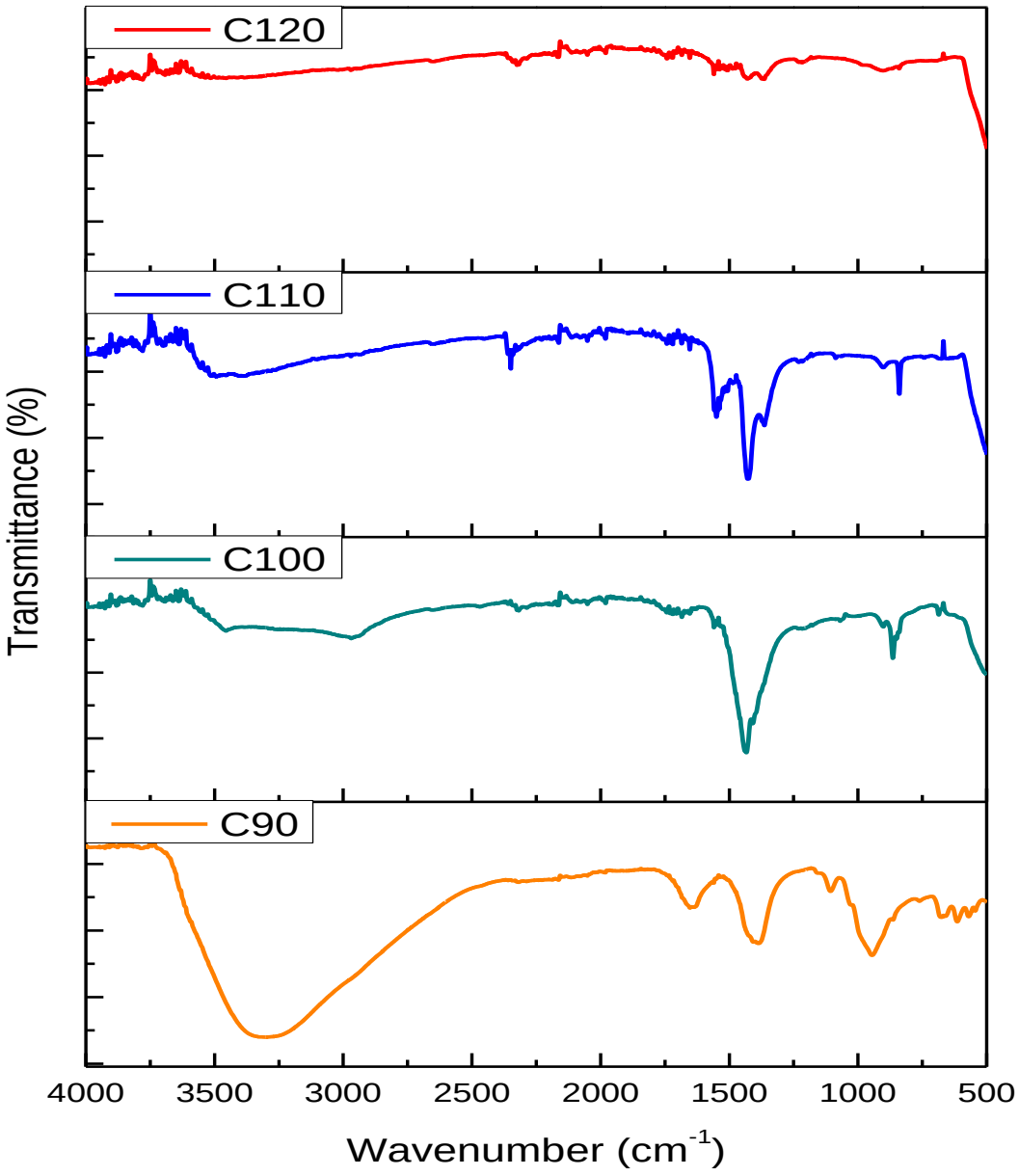

Figure 4.4: FTIR spectra of annealed Samples varying hydrothermal temperatures

4.4 Scanning Electron Microscope

The surface morphology of the samples was determined using FEI Nova NanoSEM 450.

The Figures 4.5 – 4.8 show the SEM images of the samples. The SEM images demonstrate that nearly spherical nanoparticles are produced[20]. Agglomeration of the samples was enhanced as the hydrothermal temperatures are increased in both the as-prepared and annealed samples. The enhanced agglomeration is due to the fact that surfactants were not used in this work[15].

Increasing the hydrothermal temperature and at the annealing temperature, it was observed that porosity of the materials increased. Porous materials have large surface area which helps increase light absorption.

It was also observed that well defined particles are formed when the samples were annealed at 500 ℃ for 30 minutes.

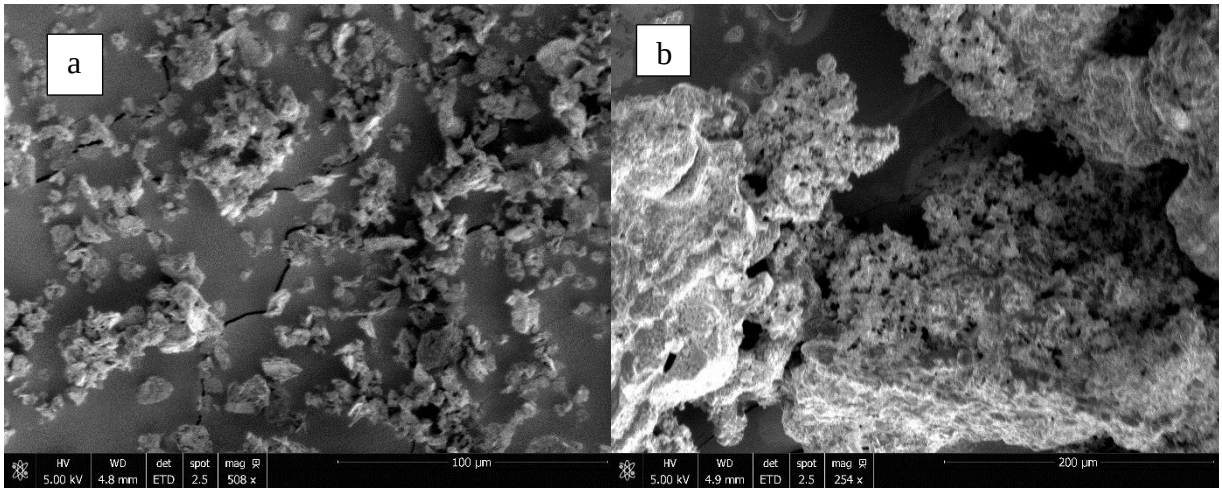

Figure 4.5: SEM of the samples hydrothermally prepared at 90 ℃ : (a) as-prepared (b) annealed at 500 ℃ for 30 minutes.

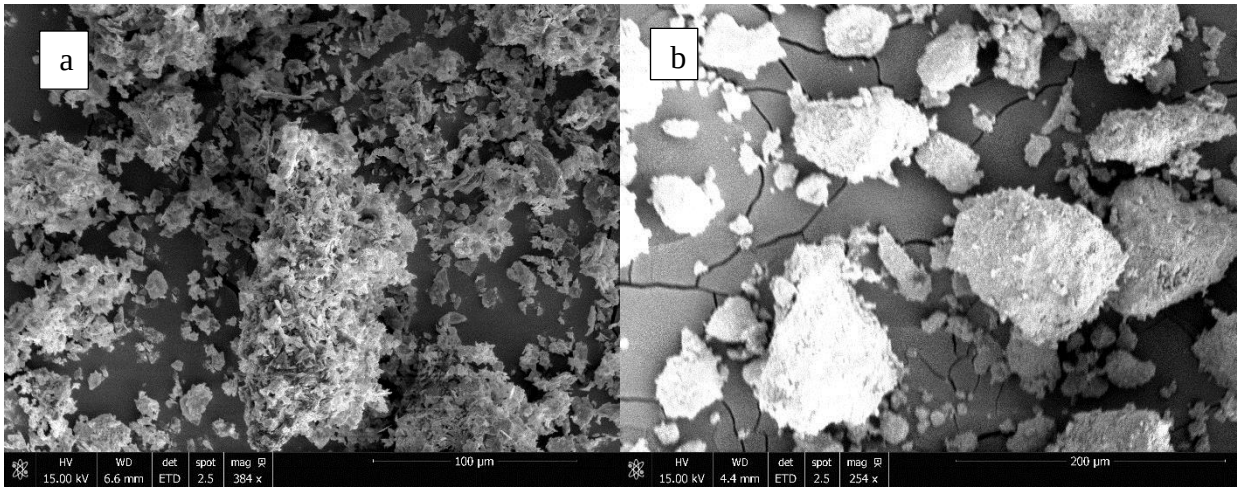

Figure 4.6 SEM of the samples hydrothermally prepared at 100 ℃ : (a) as-prepared (b) annealed at 500 ℃ for 30 minutes.

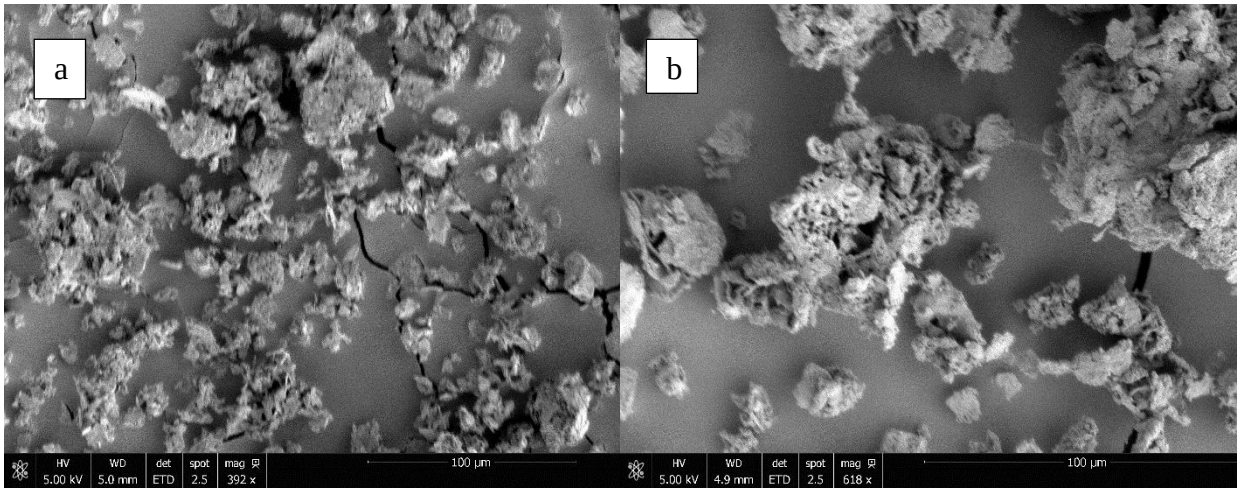

Figure 4.7: SEM of the samples hydrothermally prepared at 110 ℃ : (a) as-prepared (b) annealed at 500 ℃ for 30 minutes.

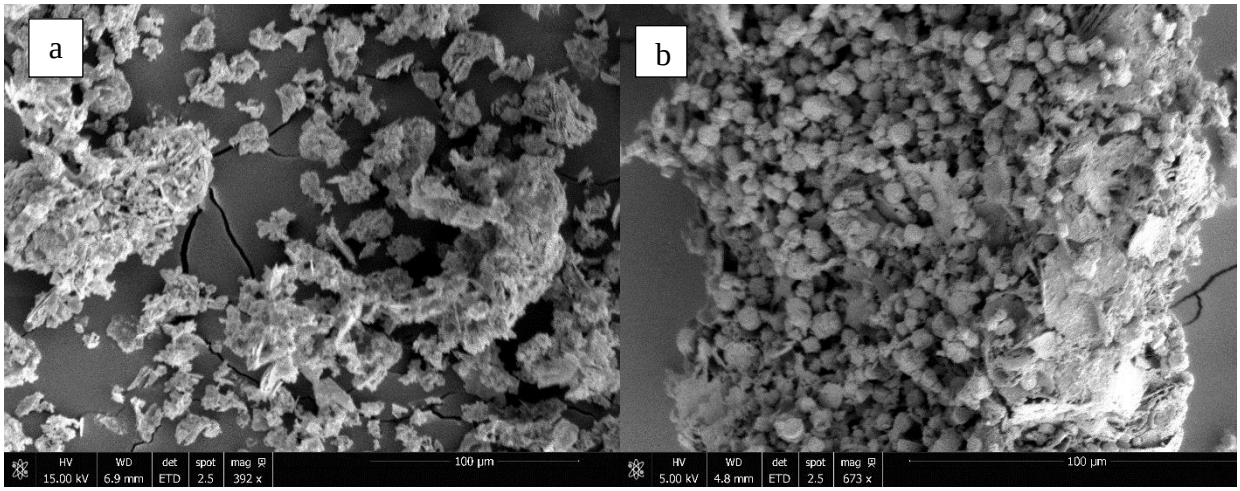

Figure 4.8: SEM of the samples hydrothermally prepared at 120 ℃ : (a) as-prepared (b) annealed at 500 ℃ for 30 minutes.

4.5 Energy Dispersive Spectroscopy(EDX)

The elemental compositions of the ZnO nanoparticles were observed using energy dispersive x-ray spectroscopy. The same peaks (for Zn and O) for all samples were observed in the EDX data confirming the formation of ZnO. All the samples were analysed on the K-series

Figure 4.9 – 4.16 show the EDX spectra of all the samples. It was observed that, increasing the hydrothermal temperature in both the as-prepared and the annealed increases the weight/atomic percent of the zinc. The unidentified peak at 2 KeV corresponds to Pt used in the sputter coating of the samples. This can be confirmed in the FTIR plots as all the organic compounds and O-H molecules disappeared with increasing hydrothermal temperature and at the annealing at 500 ℃.

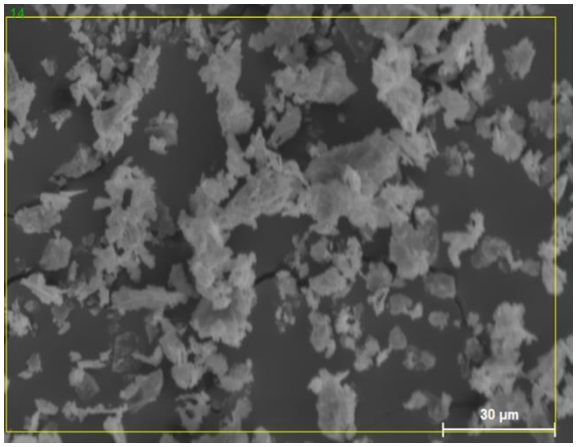

Element	Weight %	Atomic %
Zn K	71.92	38.52
O K	28.08	61.48
Total	100	100

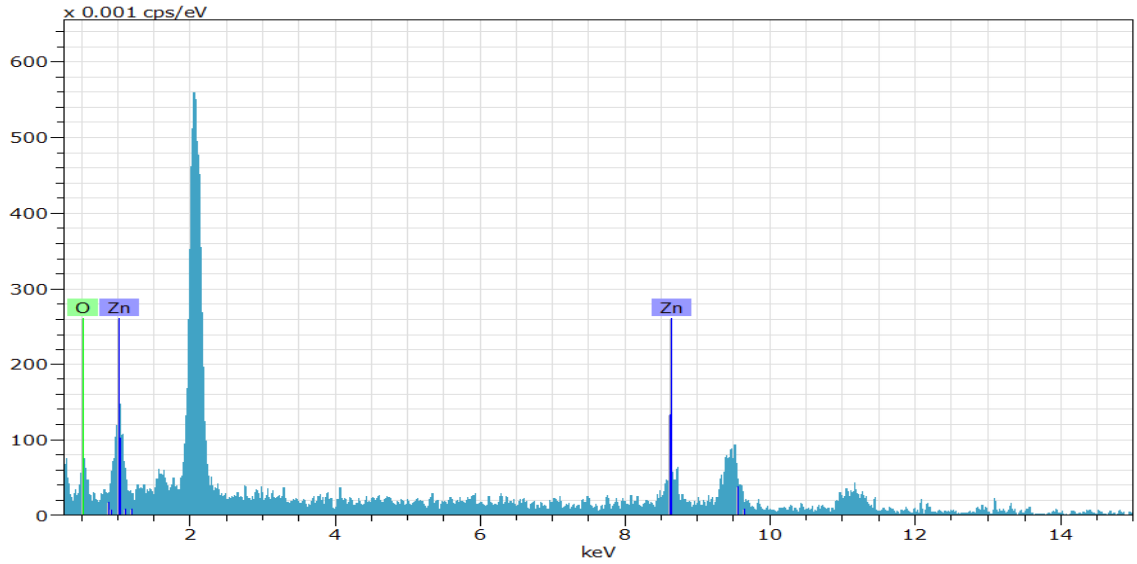

Figure 4.9: EDX of As-prepared sample at 90°C (A90)

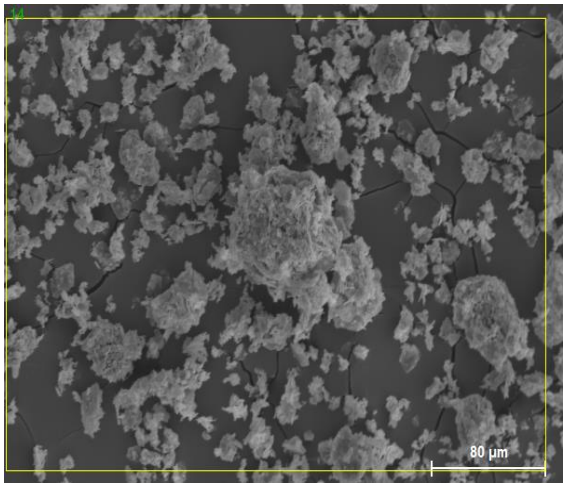

Element	Weight %	Atomic %
Zn K	73.21	40.07
O K	26.79	59.93
Total	100	100

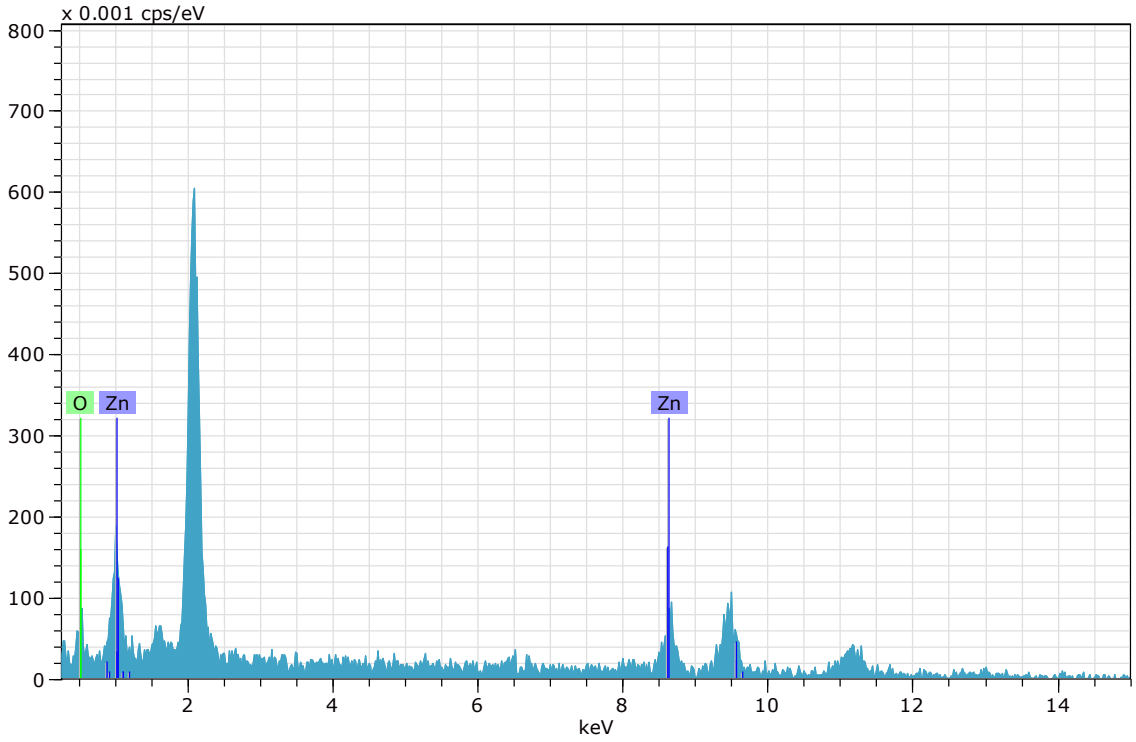

Figure 4.10: EDX of As-prepared sample at 100°C (A100)

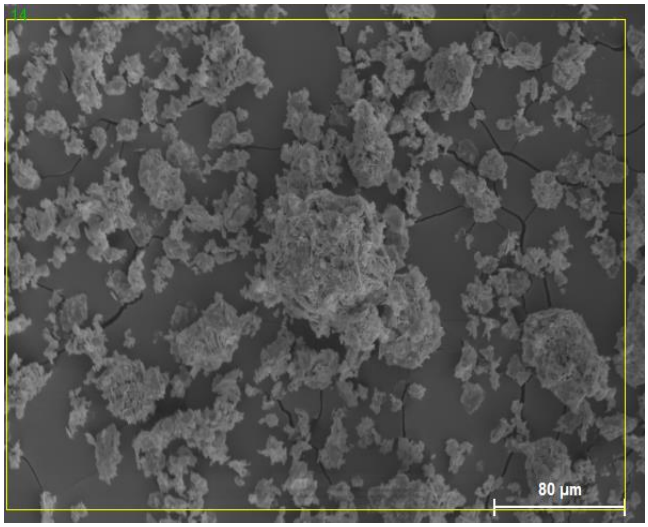

Element	Weight %	Atomic %
Zn K	73.96	41.00
O K	26.04	59.00
Total	100	100

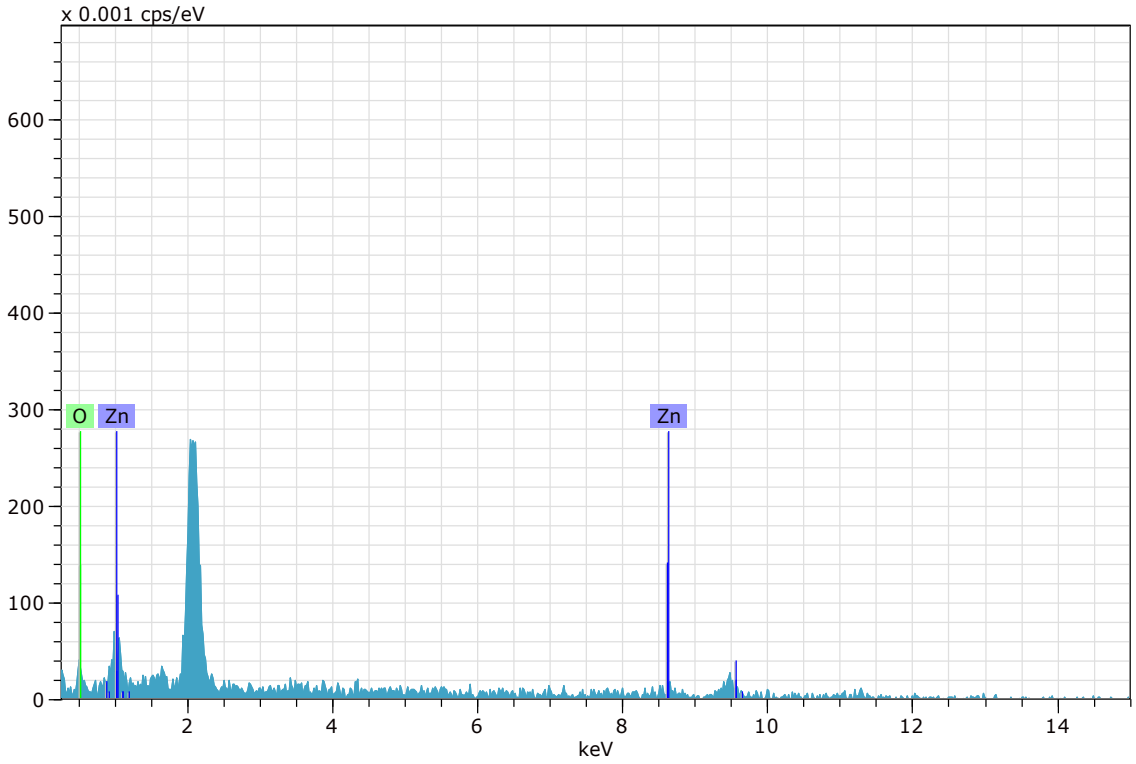

Figure 4.11: EDX of As-prepared sample at 110°C (A110)

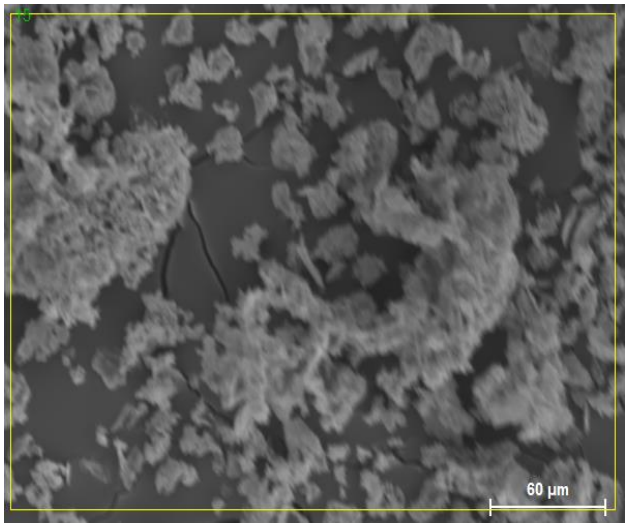

Element	Weight %	Atomic %
Zn K	78.60	47.33
O K	21.40	52.67
Total	100	100

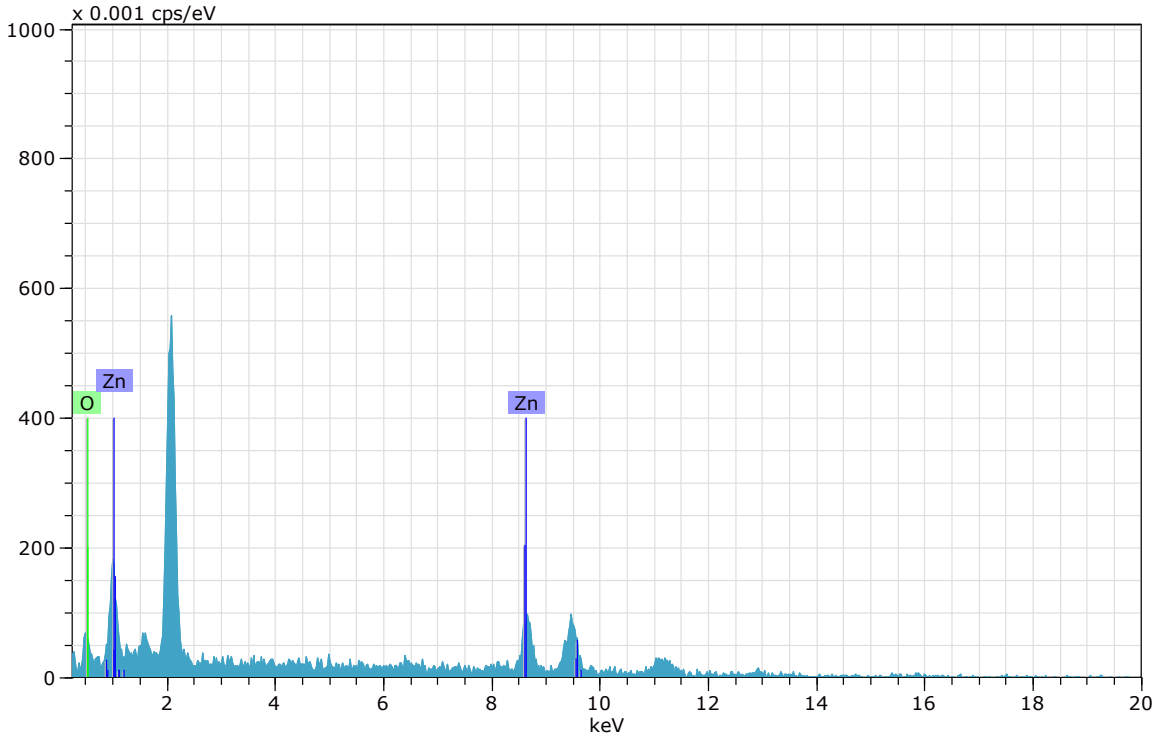

Figure 4.12: EDX of As-prepared sample at 120°C (A120)

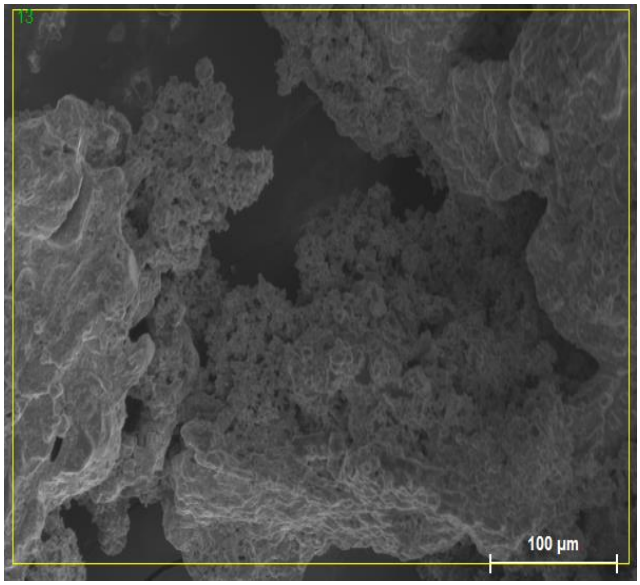

Element	Weight %	Atomic %
Zn K	75.19	92.53
O K	24.81	7.47
Total	100	100

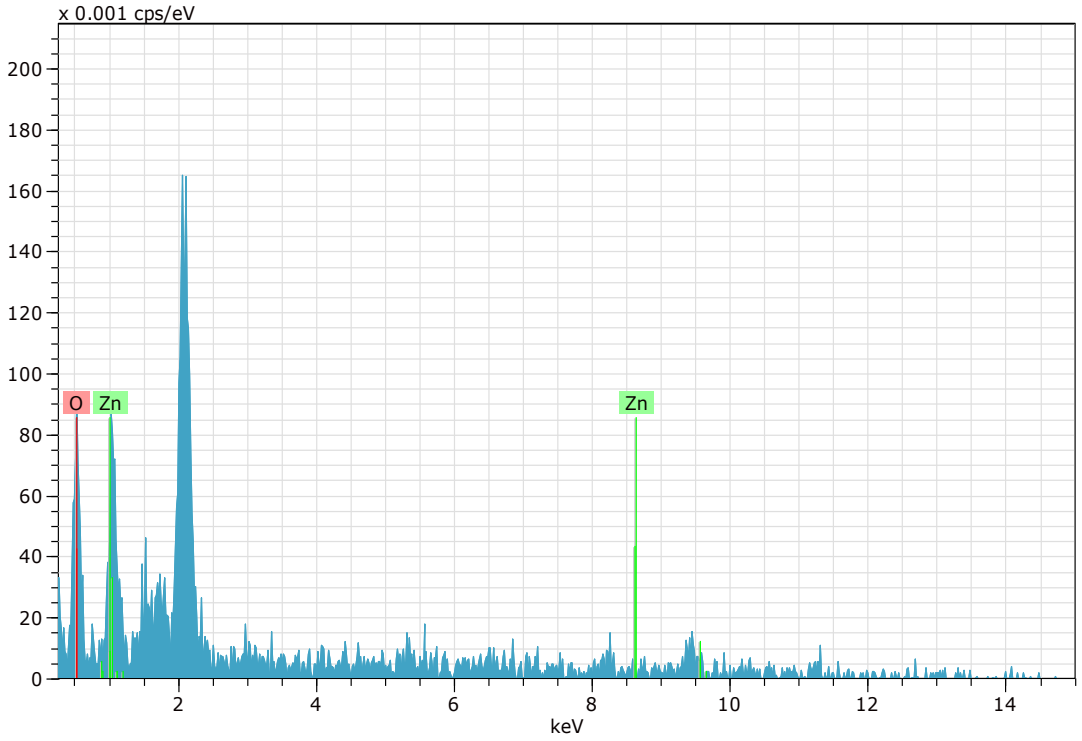

Figure 4.13: EDX of Annealed sample at hydrothermal temperature of 90 °C (C90)

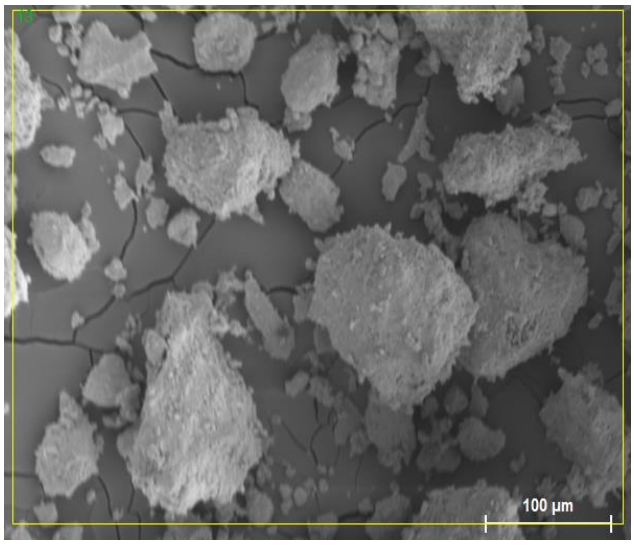

Element	Weight %	Atomic %
Zn K	84.15	56.50
O K	15.85	43.50
Total	100	100

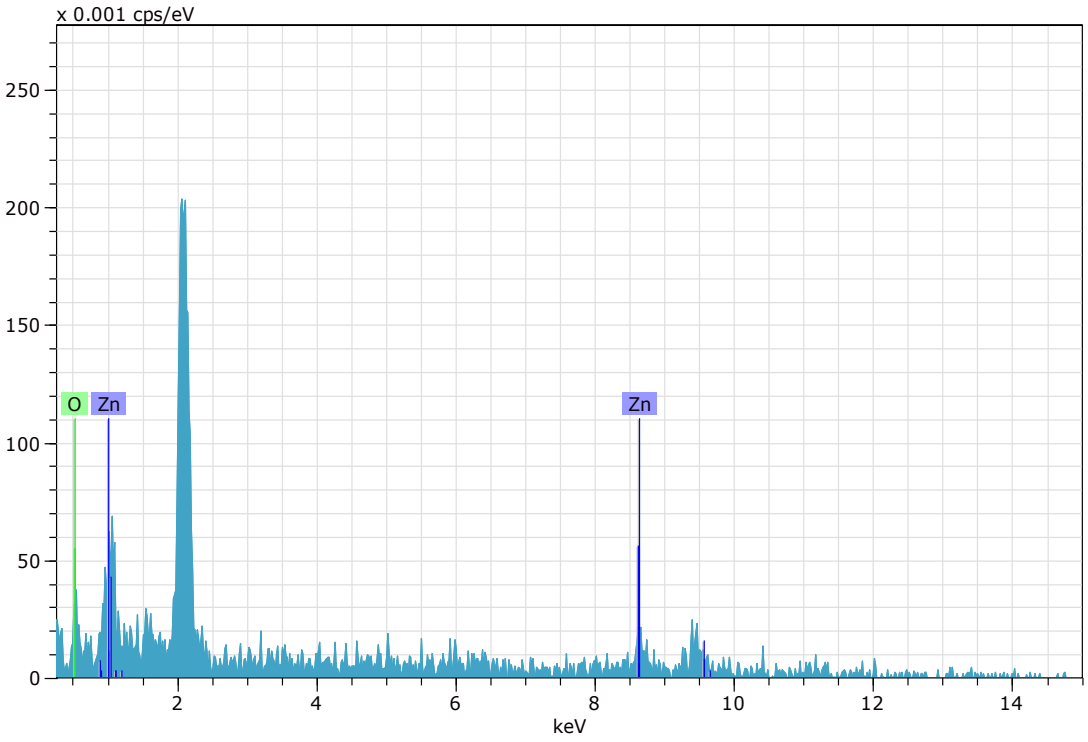

Figure .14: EDX of Annealed sample at 100 °C (C100)

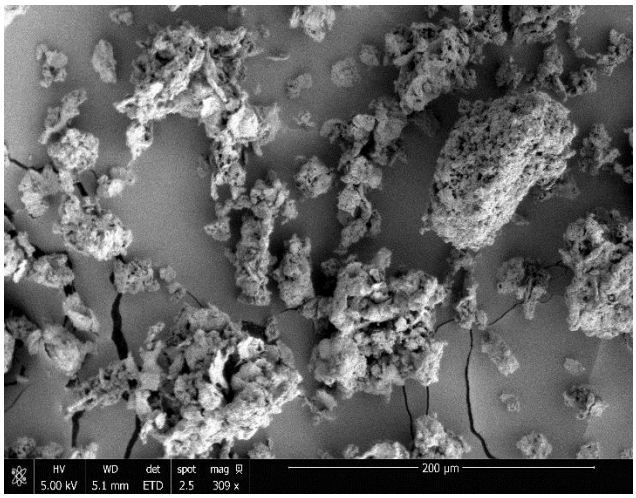

Element	Weight %	Atomic %
Zn K	86.79	61.66
O K	13.21	38.34
Total	100	100

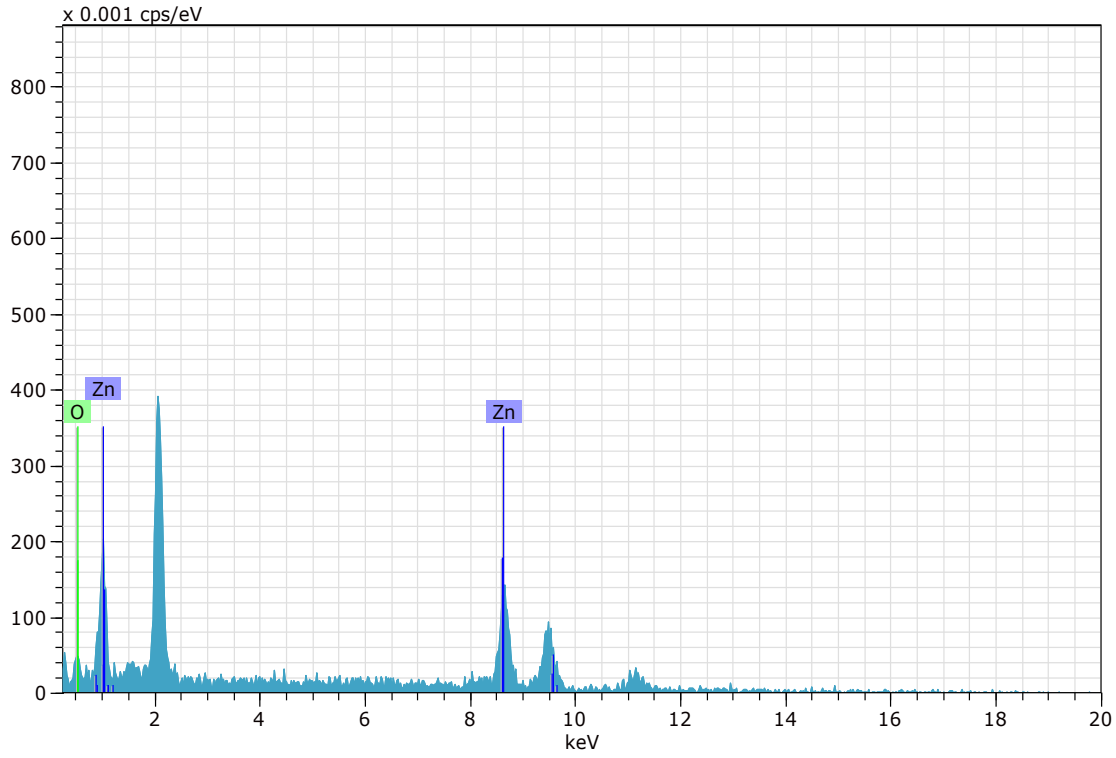

Figure 4.15: EDX of Annealed sample at 110°C (C110)

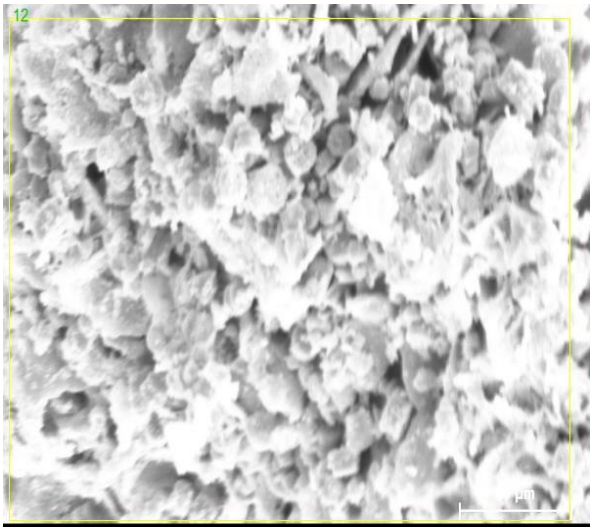

Element	Weight %	Atomic %
Zn K	89.65	67.94
O K	10.35	32.06
Total	100	100

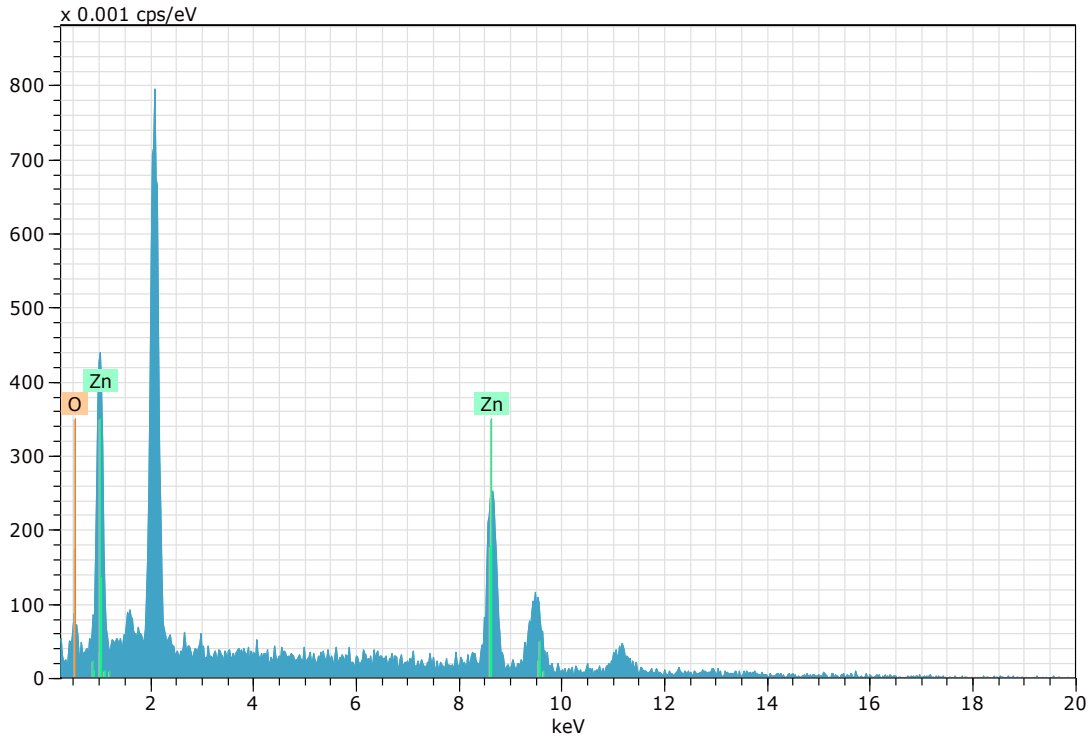

Figure 4.16: EDX of Annealed sample at 120°C (C120)

4.6 Diffuse Reflectance Spectroscopy (DRS)

The effect of the different hydrothermal temperatures on the as-grown and annealed ZnO on the optical properties of ZnO nanoparticles were investigated.

Figures 4.17- 4.22 show the diffuse reflectance and the modified Kubelka-Munk plots of the as-prepared and annealed samples. It is observed that at the annealing temperature there is a significant decrease in reflectance in all the samples. This means there is an large increase in absorption when the samples were annealed at 500 ℃ from the concept of light interaction with matter.

The large slope in the graphs of the Figures 4.17 – 4.19 indicate when all the samples start to absorb.

The absorbance has been calculated using the Kubelka-Munk equation in the limiting case of an infinitely thick sample at any wavelength[4], [24], [47], [86], [96], [97]:

$$\frac{K}{S} = \frac{(100 - R)^2}{2R} = F(R) \qquad (4.2)$$

$F(R)$ is the remission or Kubelka-Munk function (K-M). For a material which scatters in a perfectly diffuse manner, the K-M absorption coefficient K becomes equal to 2α ($K = 2\alpha$).

The band gap energy E_g and coefficient α of a direct band gap semiconductor are related through the equation

$$\alpha h\nu = B(h\nu - E_g)^{1/2} \qquad (4.3)$$

Where α is the linear absorption coefficient of the material, $h\nu$ is the photon energy and B is a proportionality constant.

Considering the K-M scattering coefficients S as a constant with respect to the wavelength and using the remission function in equation , the expression below is obtained

$$[F(R)hv]^2 = B(hv - E_g) \quad (4.4)$$

The band gap energies of the samples are measured by the extrapolation of the linear portion of the graph between the modified Kubelka-Munk (K-M) function versus photon energy (hv).

The extrapolation of the straight lines in the Figures 4.17 – 4.22 gives the value of the band gap energies.

It was found that, the optical band gap of the samples increases when they were annealed. Band gap is found to be size dependent. There is an increase in the optical band gap of the semiconductor when particle size decreases. Table 4.2 shows the optical band gaps of the as-prepared samples and the annealed samples.

The band gap of the samples did not show significant change in optical band gap when they were annealed except the sample which was hydrothermally synthesized at a temperature of 100 ℃. This observation can be attributed to quantum confinements.

The smaller band gap values in the prepared ZnO nanoparticles compared to those of bulk materials (3.3 eV) may be attributed to planar defects, like stacking faults, twin boundaries and intrinsic defects.

Table 4.2: Showing the band gap of the prepared materials.

As-prepared samples	Band gap (eV)	Annealed samples	Band gap (eV)
A100	3.11	C100	3.22
A110	3.18	C110	3.09
A120	3.16	C120	3.22

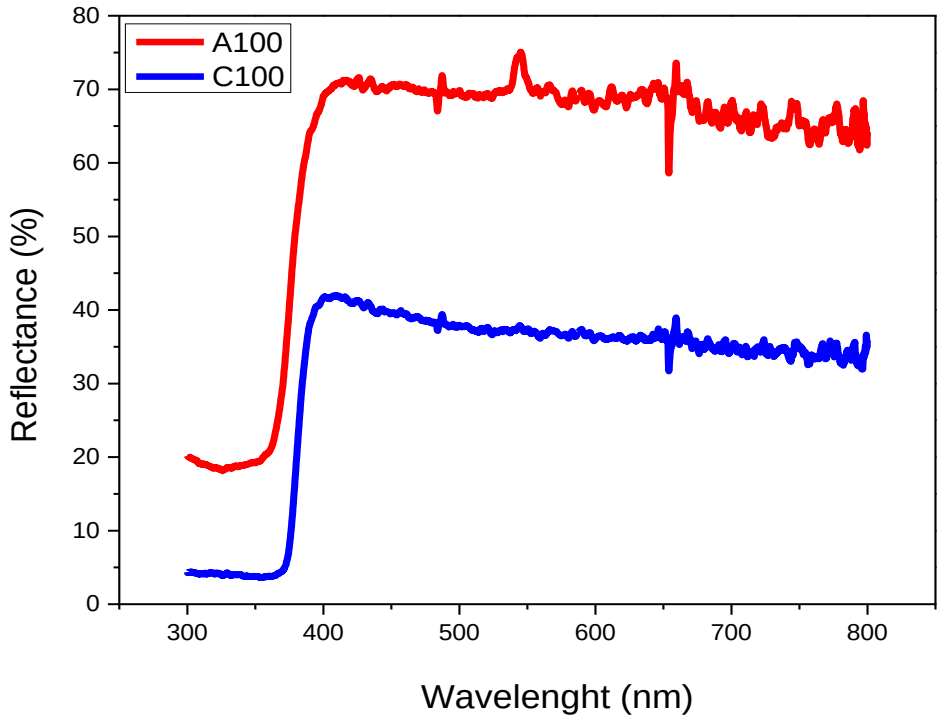

Figure 4.17: DRS of As-prepared sample A100 and Annealed sample C100

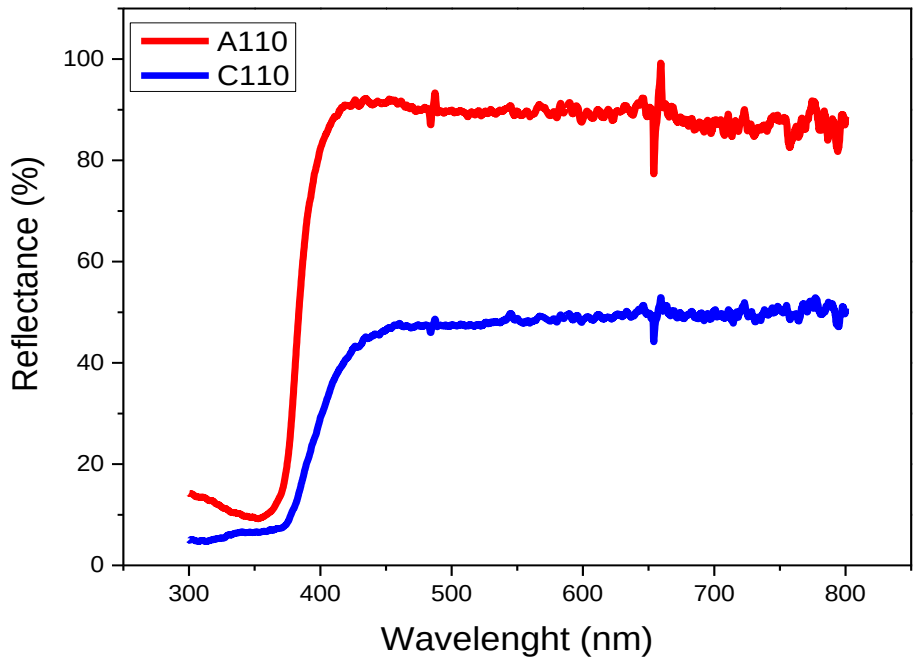

Figure 4.18: DRS of As-prepared sample A110 and Annealed sample C110

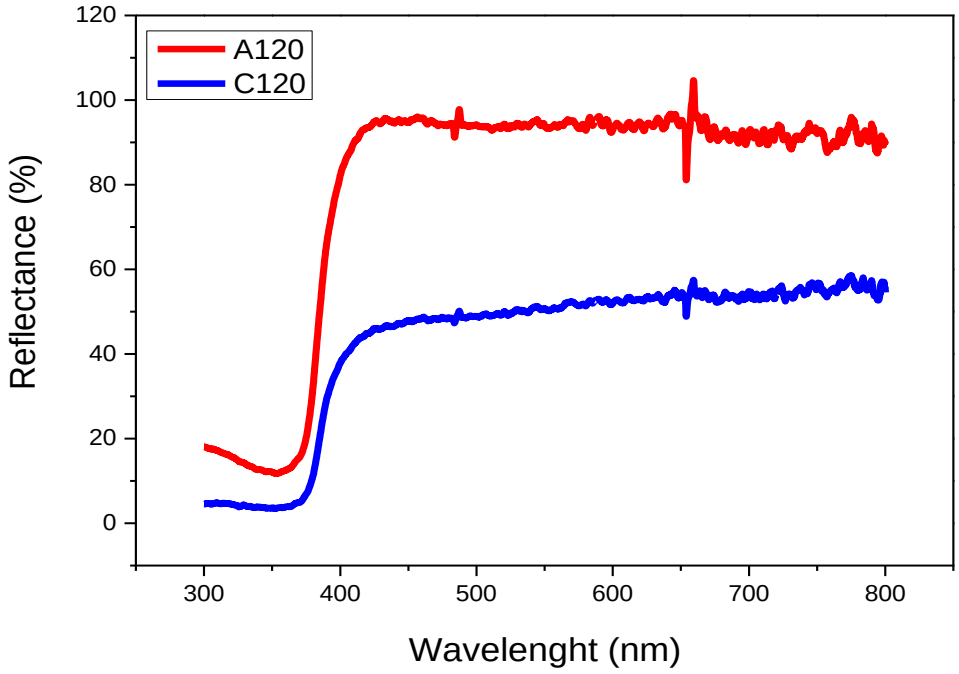

Figure 4.19: DRS of As-prepared sample A120 and Annealed sample C120

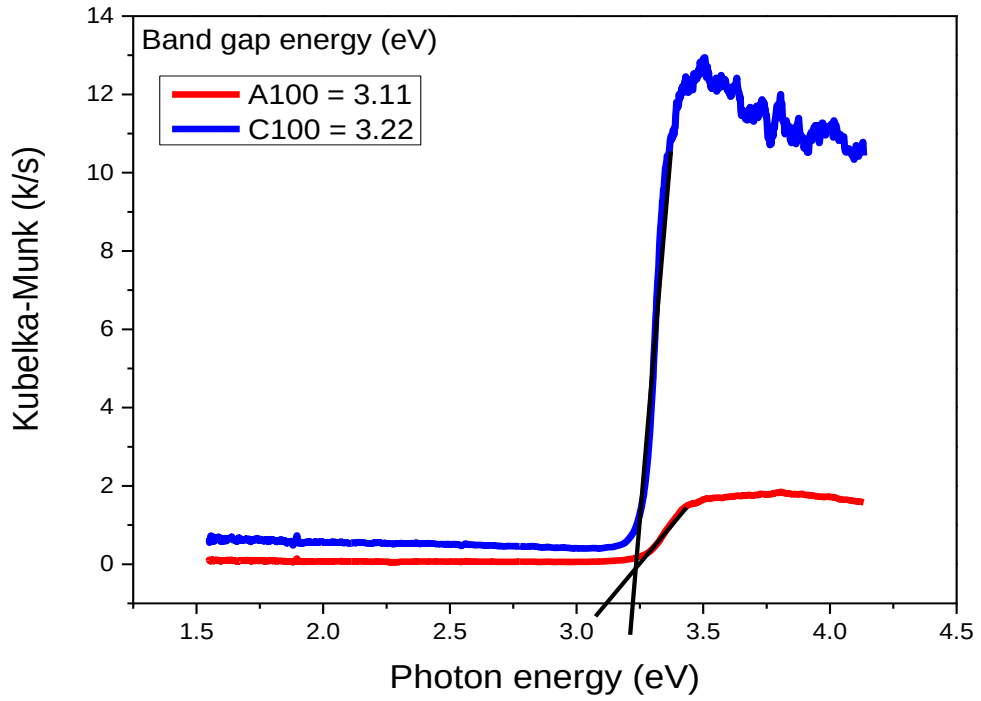

Figure 4.20 Showing the Kubelka-Munk plots of the As-prepared sample A100 and Annealed sample C100

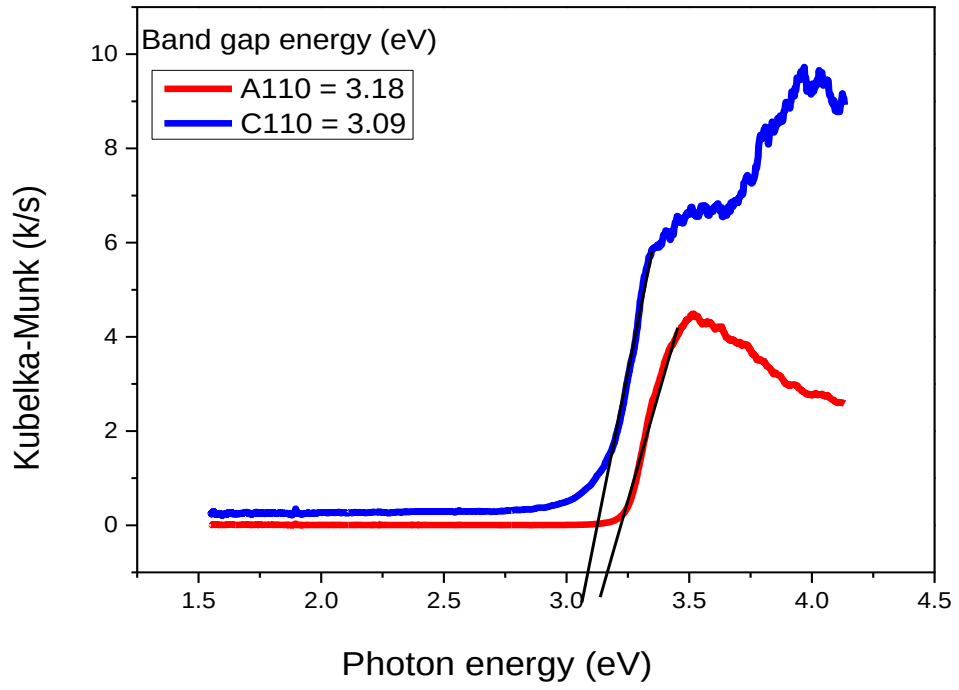

Figure 4.21: Showing the Kubelka-Munk plots of the As-prepared sample A110 and Annealed sample C110

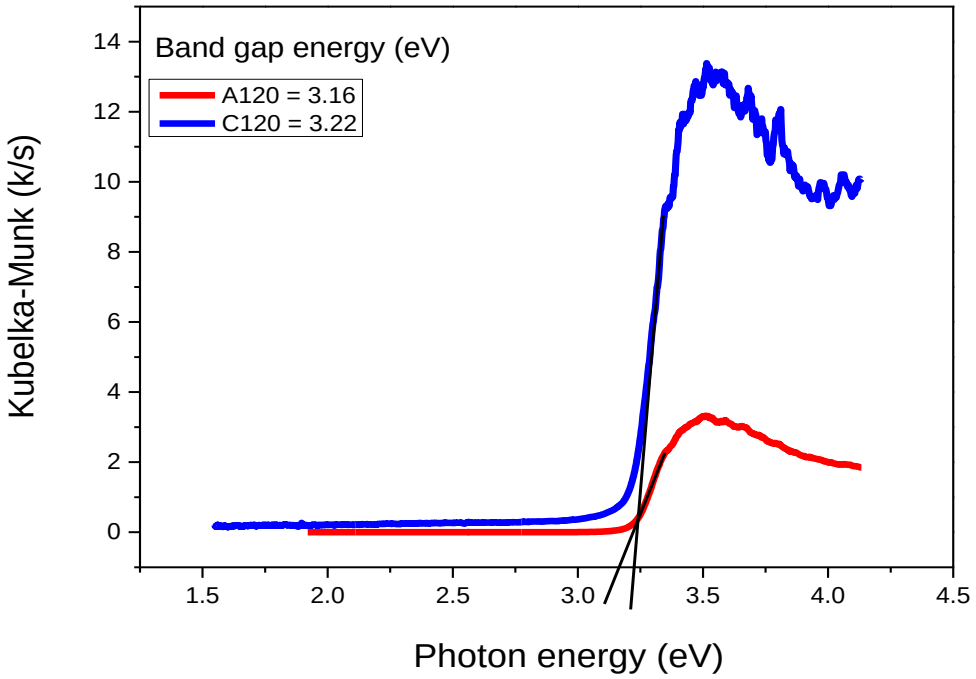

Figure 4.22: Showing the Kubelka-Munk plots of the As-prepared sample A120 and Annealed sample C120

4.7 Thermogravimetric Analysis (TGA) and Differential Scanning Calorimetry (DSC)

TGA/DSC were used to obtain the thermal properties of the samples. The results are shown in Figure 4.20- 4.23. The curves show three major discrete features.

The initial curve shows a distinct exothermic peak detected in the temperature lower than 150 ℃ with its highest band at 132 ℃ . It showed a mass loss of 13 wt. %. This exothermic peak designates basically the removal of absorbed H_2O by the samples. The distinct feature following the first curve shows a strong endothermic peak which has its maximum at the temperature 378 ℃. This feature also showed a mass loss of about 22 % which is ascribed to the combustion of all the organic compounds as a result of the zinc acetate used. The last peak cantered at 365 ℃ is due to the reduction of the layer. 32 % heat loss accompanied the whole heating process. There was no significant change observed at temperatures higher than 400 ℃. This indicates that decompositions and combustion of the organic bonds and the stability of ZnO above 400 ℃.

These are confirmed by the XRD peaks and the FTIR spectra.

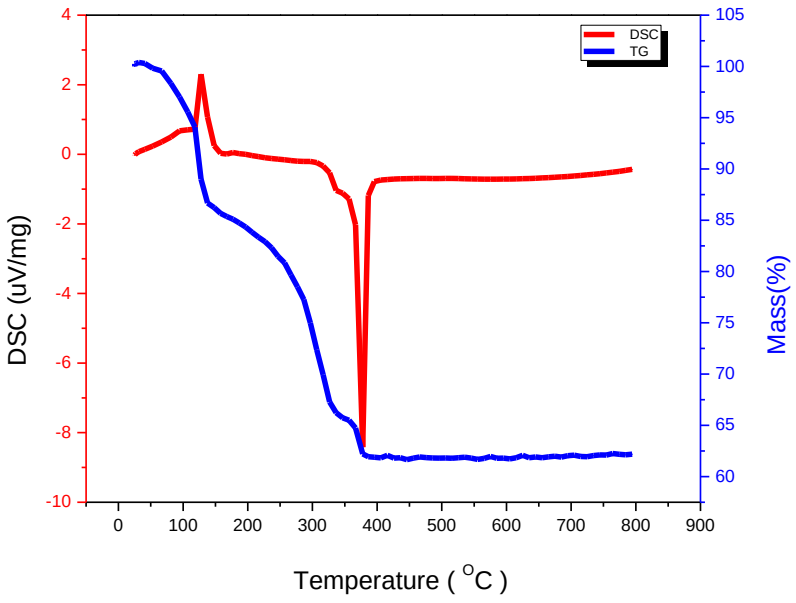

Figure 4.23:DSC/TG analysis of ZnO at hydrothermal temperature 90 ℃ (A90)

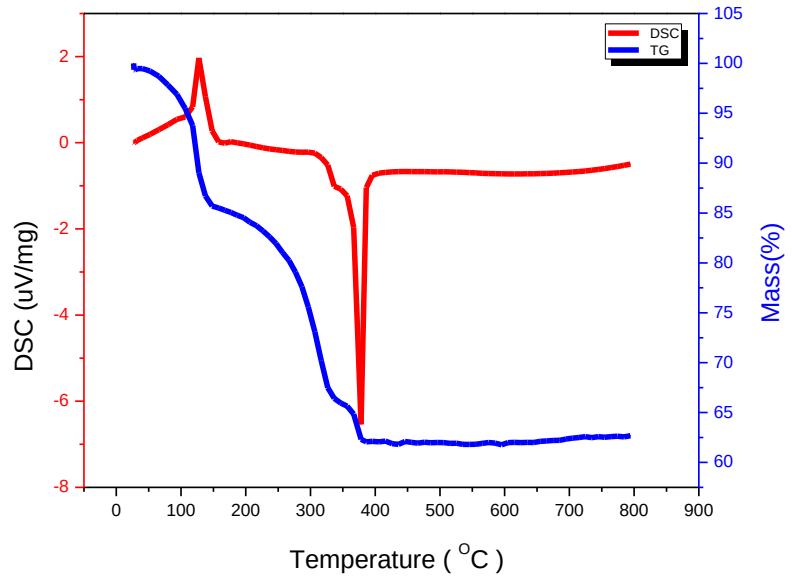

Figure 4.24: DSC/TG analysis of ZnO at hydrothermal temperature 100 ℃(A100)

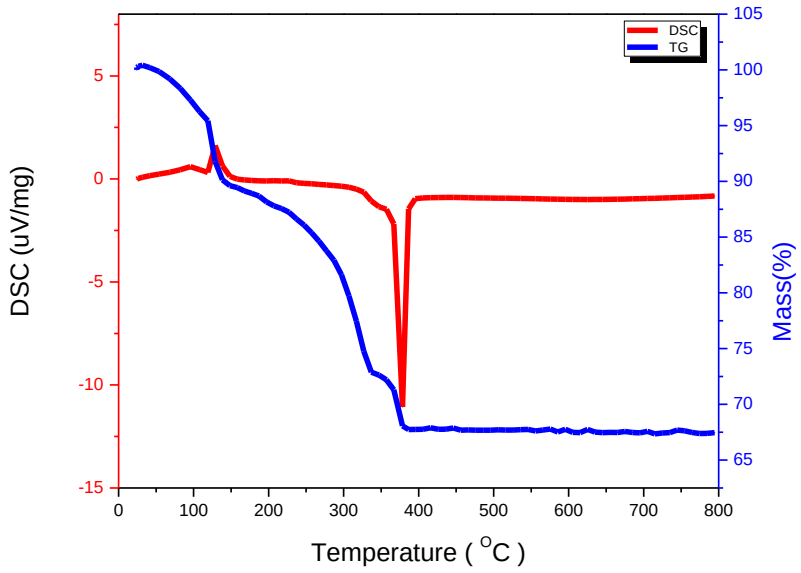

Figure 4.25: DSC/TG analysis of ZnO at hydrothermal temperature 110 ℃(A110)

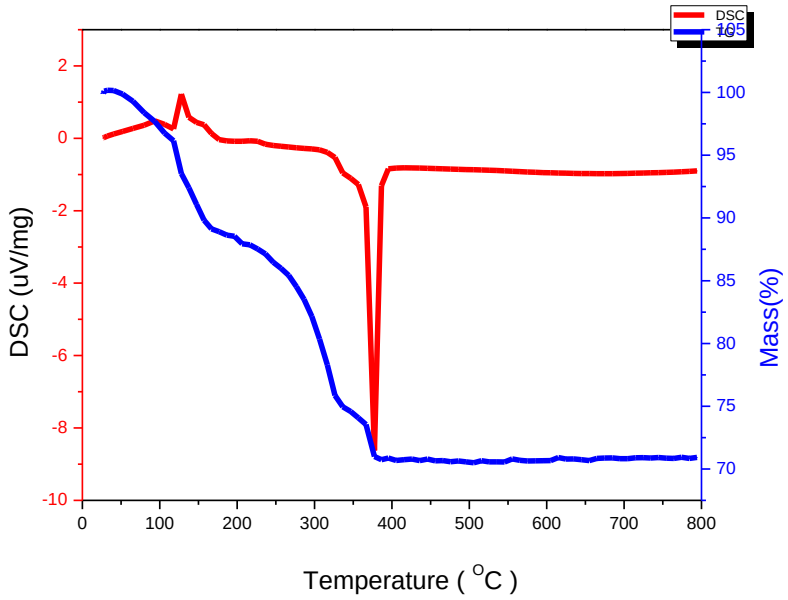

Figure 4.26: DSC/TG analysis of ZnO at hydrothermal temperature 120 ℃(A120)

CHAPTER FIVE

CONCLUSION AND RECOMMENDATION

ZnO nanoparticles were synthesized successfully by the hydrothermal technique using different hydrothermal temperatures and annealing at a temperature of 500 ℃ for 30 minutes. The synthesized nanoparticles were characterized by XRD, SEM, EDX, DRS, FTIR and TGA.

The XRD and EDX results confirm the pure, crystalline nature and hexagonal wurtzite structure of the ZnO NPs. In particular, ZnO NPs prepared by the hydrothermal treatment at 120 ℃ and annealing at 500 ℃ for 30 minutes showed the highest (002) diffraction peak as demanded for optoelectronic applications like LEDs and solar cell.

The FTIR and the DSC/TG analysis confirmed the effect of the annealing on the synthesized samples as water molecules and organic compounds present are removed with increasing hydrothermal temperature and at the annealing temperature.

The DRS results revealed that there were no drastic changes in absorption edge absorption edges for the as-prepared samples as well as the annealed samples.

The synthesized materials are recommended for solar cell and other optoelectronic applications since the dominant (002) diffraction peak of the hydrothermally synthesized material at the annealing temperature of 500 ℃ for 30 minutes is very crucial for optoelectronic applications. This is due to the fact that electrons travelling in the solar cell prefer to travel on the (002) plane.

REFERENCES

[1] K. Ranabhat, L. Patrikeev, A. Antal'evna-Revina, K. Andrianov, V. Lapshinsky, and E. Sofronova, "An introduction to solar cell technology," *Istraz. i Proj. za privredu*, vol. 14, no. 4, pp. 481–491, 2016.

[2] V. Khare, S. Nema, and P. Baredar, "Status of solar wind renewable energy in India," *Renew. Sustain. Energy Rev.*, vol. 27, pp. 1–10, 2013.

[3] P. Sinsermsuksakul, R. Chakraborty, S. B. Kim, S. M. Heald, T. Buonassisi, and R. G. Gordon, "Antimony-doped tin(II) sulfide thin films," *Chem. Mater.*, vol. 24, no. 23, pp. 4556–4562, 2012.

[4] D. N. Papadimitriou, G. Roupakas, G. G. Roumeliotis, P. Vogt, and T. Köhler, "Optimization of electrochemically deposited highly doped ZnO bilayers on ga-rich chalcopyrite selenide for cost-effective photovoltaic device technology," *Energies*, vol. 9, no. 11, 2016.

[5] K. I. Bogutska, Y. P. Sklyarov, and Y. I. Prylutskyy, "Zinc and zinc nanoparticles : biological role and application in biomedicine," vol. 1, pp. 9–16, 2013.

[6] M. Zi, M. Zhu, L. Chen, H. Wei, X. Yang, and B. Cao, "ZnO photoanodes with different morphologies grown by electrochemical deposition and their dye-sensitized solar cell properties," *Ceram. Int.*, vol. 40, no. 6, pp. 7965–7970, 2014.

[7] H. Chou and H. Hsu, "Solid-State Electronics The effect of annealing temperatures to prepare ZnO seeds layer on ZnO nanorods array / TiO 2 nanoparticles photoanode," *Solid State Electron.*, vol. 116, pp. 15–21, 2016.

[8] A. M. Hussein, A. V. Iefanova, R. T. Koodali, B. A. Logue, and R. V. Shende, "Interconnected ZrO2doped ZnO/TiO2network photoanode for dye-sensitized solar

cells," *Energy Reports*, vol. 4, pp. 56–64, 2018.

[9] S. N. Sadikin, M. Y. A. Rahman, and A. A. Umar, "TiO 2 - BaTiO 3 Composite Films as Photoanode for Dye Sensitized Solar Cell : Effect of BaTiO 3 Content," vol. 113, no. November, pp. 109–113, 2017.

[10] S. K. Park and Y. S. Han, "Efficient dye-sensitized solar cells with surface-modified photoelectrodes," *Sol. Energy*, vol. 110, pp. 260–267, 2014.

[11] M. Ye *et al.*, "Recent advances in dye-sensitized solar cells: From photoanodes, sensitizers and electrolytes to counter electrodes," *Mater. Today*, vol. 18, no. 3, pp. 155–162, 2015.

[12] D. Tahir and K. H. Jae, "Effect of growth temperature on structural and electronic properties of ZnO thin films," vol. 020007, p. 020007, 2017.

[13] L. Lu, R. Li, K. Fan, and T. Peng, "Effects of annealing conditions on the photoelectrochemical properties of dye-sensitized solar cells made with ZnO nanoparticles," *Sol. Energy*, vol. 84, no. 5, pp. 844–853, 2010.

[14] C. Y. Jiang, X. W. Sun, G. Q. Lo, D. L. Kwong, and J. X. Wang, "Improved dye-sensitized solar cells with a ZnO-nanoflower photoanode," *Appl. Phys. Lett.*, vol. 90, no. 26, 2007.

[15] "Applied Catalysis A : General," no. March, 2016.

[16] J. Wu, G. Chen, H. Yang, C. Ku, and J. Lai, "Effects of dye adsorption on the electron transport properties in ZnO-nanowire dye-sensitized solar cells," pp. 2007–2009, 2007.

[17] J. Lee, A. J. Easteal, U. Pal, and D. Bhattacharyya, "Evolution of ZnO nanostructures in sol – gel synthesis," *Curr. Appl. Phys.*, vol. 9, no. 4, pp. 792–796, 2009.

[18] A. Kołodziejczak-radzimska and T. Jesionowski, "Zinc Oxide—From Synthesis to Application: A Review," pp. 2833–2881, 2014.

[19] H. Xu *et al.*, "Hydrothermal synthesis of zinc oxide powders with controllable morphology," vol. 30, pp. 93–97, 2004.

[20] S. R. Brintha and M. Ajitha, "Synthesis and characterization of ZnO nanoparticles via aqueous solution , sol-gel and hydrothermal methods," vol. 8, no. 11, pp. 66–72, 2015.

[21] L. Znaidi, "Sol-gel-deposited ZnO thin films: A review," *Mater. Sci. Eng. B Solid-State Mater. Adv. Technol.*, vol. 174, no. 1–3, pp. 18–30, 2010.

[22] T. Makino, Y. Segawa, M. Kawasaki, and H. Koinuma, "Optical properties of excitons in ZnO-based quantum well heterostructures," *Semicond. Sci. Technol.*, vol. 20, no. 4, 2005.

[23] C. H. Lu and C. H. Yeh, "Influence of hydrothermal conditions on the morphology and particle size of zinc oxide powder," *Ceram. Int.*, vol. 26, no. 4, pp. 351–357, 2000.

[24] R. Raji and K. G. Gopchandran, "ZnO nanostructures with tunable visible luminescence: Effects of kinetics of chemical reduction and annealing," *J. Sci. Adv. Mater. Devices*, vol. 2, no. 1, pp. 51–58, 2017.

[25] R. R. Hong, R. Hong, T. Pan, J. Qian, and H. Li, "Synthesis and Surface Modification of ZnO Nanoparticles Synthesis and surface modification of ZnO nanoparticles," no. March, 2016.

[26] P. C. Æ. W. J. Song, "Preparation of ZnO Nanoparticles by a Surfactant-Assisted Complex Sol-Gel Method Using Zinc Nitrate complex sol – gel method using zinc nitrate," no. AUGUST, 2009.

[27] M. Izaki, T. Shinagawa, and K. Mizuno, "Electrochemically constructed p-Cu 2 O / n-

ZnO heterojunction diode for photovoltaic device," 2007.

[28] D. A. M. Osman and M. A. Mustafa, "Synthesis and Characterization of Zinc Oxide Nanoparticles using Zinc Acetate Dihydrate and Sodium Hydroxide Synthesis and Characterization of Zinc Oxide Nanoparticles using Zinc Acetate Dihydrate and Sodium Hydroxide," *J. Nanosci. Nanoeng.*, vol. 1, no. 4, pp. 248–251, 2015.

[29] A. Khorsand Zak, R. Razali, W. H. Abd Majid, and M. Darroudi, "Synthesis and characterization of a narrow size distribution of zinc oxide nanoparticles," *Int. J. Nanomedicine*, vol. 6, no. 1, pp. 1399–1403, 2011.

[30] J. E. Boercker, S. M. Mahpeykar, and J. Koohsorkhi, "Synthesis and characterization of ZnO nanowires and their integration into dye-sensitized solar cells," 2006.

[31] A. Erol, S. Okur, B. Comba, ?? Mermer, and M. ?? Arikan, "Humidity sensing properties of ZnO nanoparticles synthesized by sol-gel process," *Sensors Actuators, B Chem.*, vol. 145, no. 1, pp. 174–180, 2010.

[32] T. M. Hammad, J. K. Salem, and R. G. Harrison, "The influence of annealing temperature on the structure, morphologies and optical properties of ZnO nanoparticles," *Superlattices Microstruct.*, vol. 47, no. 2, pp. 335–340, 2010.

[33] J. Ungula, B. F. Dejene, and H. C. Swart, "Effect of annealing on the structural, morphological and optical properties of Ga-doped ZnO nanoparticles by reflux precipitation method," *Results Phys.*, vol. 7, pp. 2022–2027, 2017.

[34] L. Schmidt-Mende and J. L. MacManus-Driscoll, "ZnO - nanostructures, defects, and devices," *Mater. Today*, vol. 10, no. 5, pp. 40–48, 2007.

[35] L. Lin *et al.*, "Correlation between native defects and morphological, structural and optical properties of ZnO nanostructures," *J. Alloys Compd.*, vol. 695, pp. 1523–1527,

2017.

[36] K. Liu, M. Sakurai, and M. Aono, "ZnO-based ultraviolet photodetectors," *Sensors*, vol. 10, no. 9, pp. 8604–8634, 2010.

[37] J. D. Roy-Mayhew and I. A. Aksay, "Graphene materials and their use in dye-sensitized solar cells," *Chem Rev*, vol. 114, no. 12, pp. 6323–6348, 2014.

[38] Y. Zhang, M. K. Ram, E. K. Stefanakos, and D. Y. Goswami, "Synthesis , Characterization , and Applications of ZnO Nanowires," no. December, 2015.

[39] I. Khan, K. Saeed, and I. Khan, "Nanoparticles : Properties , applications and toxicities," *Arab. J. Chem.*, 2017.

[40] M. Y. Ge *et al.*, "Nanostructured ZnO: From monodisperse nanoparticles to nanorods," *J. Cryst. Growth*, vol. 305, no. 1, pp. 162–166, 2007.

[41] Q. H. Wang, K. Kalantar-Zadeh, A. Kis, J. N. Coleman, and M. S. Strano, "Electronics and optoelectronics of two-dimensional transition metal dichalcogenides," *Nat. Nanotechnol.*, vol. 7, no. 11, pp. 699–712, 2012.

[42] F. B. Dejene *et al.*, "Optical properties of ZnO nanoparticles synthesized by varying the sodium hydroxide to zinc acetate molar ratios using a Sol-Gel process," *Cent. Eur. J. Phys.*, vol. 9, no. 5, pp. 1321–1326, 2011.

[43] A. Janotti and C. G. Van De Walle, "Fundamentals of zinc oxide as a semiconductor," vol. 72, 2009.

[44] A. K. Zak, W. H. A. Majid, M. Darroudi, and R. Yousefi, "Synthesis and characterization of ZnO nanoparticles prepared in gelatin media," *Mater. Lett.*, vol. 65, no. 1, pp. 70–73, 2011.

[45] K. Okuyama and I. W. Lenggoro, "Preparation of Nanoparticles Via Spray Route Preparation of nanoparticles via spray route," vol. 2509, no. MARCH 2003, 2016.

[46] T. Gordon, B. Perlstein, O. Houbara, I. Felner, E. Banin, and S. Margel, "Colloids and Surfaces A : Physicochemical and Engineering Aspects Synthesis and characterization of zinc / iron oxide composite nanoparticles and their antibacterial properties," *Colloids Surfaces A Physicochem. Eng. Asp.*, vol. 374, no. 1–3, pp. 1–8, 2011.

[47] A. K. Zak, M. E. Abrishami, W. H. A. Majid, R. Yousefi, and S. M. Hosseini, "Effects of annealing temperature on some structural and optical properties of ZnO nanoparticles prepared by a modified sol-gel combustion method," *Ceram. Int.*, vol. 37, no. 1, pp. 393–398, 2011.

[48] R. M. Alwan *et al.*, "Synthesis of Zinc Oxide Nanoparticles via Sol – Gel Route and Their Characterization," *Nanosci. Nanotechnol.*, vol. 5, no. 1, pp. 1–6, 2015.

[49] Z. L. Wang, "Zinc oxide nanostructures: Growth, properties and applications," *J. Phys. Condens. Matter*, vol. 16, no. 25, 2004.

[50] H. Morkoc and U. Ozgur, *General Properties of ZnO*. 2009.

[51] P. S. Sokolov, A. N. Baranov, Z. V. Dobrokhotova, and V. L. Solozhenkoa, "Synthesis and thermal stability of cubic ZnO in the salt nanocomposites," *Russ. Chem. Bull.*, vol. 59, no. 2, pp. 325–328, 2010.

[52] A. Ashrafi and C. Jagadish, "Review of zincblende ZnO: Stability of metastable ZnO phases," *J. Appl. Phys.*, vol. 102, no. 7, 2007.

[53] A. K. Zak, "Effects of annealing temperature on some structural and optical properties of ZnO nanoparticles prepared by a modified sol – gel combustion method," no. March, 2016.

[54] P. J. P. Espitia, N. de F. F. Soares, J. S. dos R. Coimbra, N. J. de Andrade, R. S. Cruz, and E. A. A. Medeiros, "Zinc Oxide Nanoparticles: Synthesis, Antimicrobial Activity and Food Packaging Applications," *Food Bioprocess Technol.*, vol. 5, no. 5, pp. 1447–1464, 2012.

[55] Y. Ding, K. C. Pradel, and Z. L. Wang, "In situ transmission electron microscopy observation of ZnO polar and non-polar surfaces structure evolution under electron beam irradiation," *J. Appl. Phys.*, vol. 119, no. 1, 2016.

[56] Y. Ding, Z. L. Wang, T. Sun, and J. Qiu, "Zinc-blende ZnO and its role in nucleating wurtzite tetrapods and twinned nanowires," *Appl. Phys. Lett.*, vol. 90, no. 15, pp. 3–5, 2007.

[57] V. Kumar, O. M. Ntwaeaborwa, T. Soga, V. Dutta, and H. C. Swart, "Rare Earth Doped Zinc Oxide Nanophosphor Powder: A Future Material for Solid State Lighting and Solar Cells," *ACS Photonics*, vol. 4, no. 11, pp. 2613–2637, 2017.

[58] C. Wo, "The chemistry and physics of zinc oxide surfaces," vol. 82, pp. 55–120, 2007.

[59] M. Willander *et al.*, "Luminescence from zinc oxide nanostructures and polymers and their hybrid devices," *Materials (Basel).*, vol. 3, no. 4, pp. 2643–2667, 2010.

[60] B. Meyer, "First-principles study of the polar O-terminated ZnO surface in thermodynamic equilibrium with oxygen and hydrogen," *Phys. Rev. B - Condens. Matter Mater. Phys.*, vol. 69, no. 4, pp. 1–10, 2004.

[61] B. Meyer and D. Marx, "Density-functional study of the structure and stability of ZnO surfaces," 2002.

[62] O. Fruchart, A. Masseboeuf, J. C. Toussaint, and P. Bayle-Guillemaud, "Growth and micromagnetism of self-assembled epitaxial fcc(111) cobalt dots," *J. Phys. Condens.*

Matter, vol. 25, no. 49, pp. 1–8, 2013.

[63] X. Y. Kong and Z. L. Wang, "Polar-surface dominated ZnO nanobelts and the electrostatic energy induced nanohelixes, nanosprings, and nanospirals," *Appl. Phys. Lett.*, vol. 84, no. 6, pp. 975–977, 2004.

[64] C. R. Bhattacharjee, D. D. Purkayastha, S. Bhattacharjee, and A. Nath, "Homogeneous Chemical Precipitation Route to ZnO Nanospherical s," pp. 122–127, 2011.

[65] T. Kakhia, "2.1 Physical."

[66] P. Verma, S. Pandey, and A. C. Pandey, "Synthesis and photoluminescence of ZnO Nanophosphors," *Thin Solid Films*, pp. 256–258.

[67] S. Patil and S. J. Raut, "SYNTHESIS AND CHARACTERIZATION OF ZnO NANOPARTICLES AND 50 % ZnO-BENTONITE NANOCOMPOSITE," vol. 10, no. 2, pp. 1124–1132, 2012.

[68] A. Janotti, J. B. Varley, J. L. Lyons, and C. G. Van De Walle, "Functional Metal Oxide Nanostructures," vol. 149, 2012.

[69] L. Liu *et al.*, "Oxygen vacancies: The origin of <math> <mi>n</mi> </math> -type conductivity in ZnO," *Phys. Rev. B*, vol. 93, no. 23, p. 235305, 2016.

[70] D. F. Urban, W. Körner, and C. Elsässer, "Mechanisms for p-type behavior of ZnO, Zn$_{1-x}$Mg$_x$O and related oxide semiconductors," pp. 1–7, 2016.

[71] J. W. Sun *et al.*, "Excitonic electroluminescence from ZnO-based heterojunction light emitting diodes," *J. Phys. D. Appl. Phys.*, vol. 41, no. 15, 2008.

[72] P. Rodnyi and I. Khodyuk, "Optical and luminescence properties of zinc oxide (Review)," *Opt. Spectrosc.*, vol. 111, no. 5, pp. 776–785, 2011.

[73] A. A. High, A. T. Hammack, L. V. Butov, M. Hanson, and A. C. Gossard, "Exciton optoelectronic transistor," *Opt. Lett.*, vol. 32, no. 17, p. 2466, 2007.

[74] Y. Y. Kuznetsova *et al.*, "All-optical excitonic transistor.," *Opt. Lett.*, vol. 35, no. 10, pp. 1587–9, 2010.

[75] G. Grosso *et al.*, "Excitonic switches operating at around 100K," *Nat. Photonics*, vol. 3, no. 10, pp. 577–580, 2009.

[76] H. Zeng, G. Duan, Y. Li, S. Yang, X. Xu, and W. Cai, "Blue luminescence of ZnO nanoparticles based on non-equilibrium processes: Defect origins and emission controls," *Adv. Funct. Mater.*, vol. 20, no. 4, pp. 561–572, 2010.

[77] Y. Kim and S. Kang, "Calculation of Formation Energy of Oxygen Vacancy in ZnO Based on Photoluminescence Measurements," *J. Phys. Chem. B*, vol. 114, no. 23, pp. 7874–7878, 2010.

[78] S. S. Kumar, P. Venkateswarlu, V. R. Rao, and G. N. Rao, "Synthesis , characterization and optical properties of zinc oxide nanoparticles," pp. 1–6, 2013.

[79] V. T. Bhugul and G. N. Choudhari, "Synthesis and Studies on Nanocomposites of polypyrrole- Al- doped zinc oxide Nanoparticles," *Int. J. Sci. Res. Publ.*, vol. 5, no. 1, pp. 1–5, 2015.

[80] M. Niederberger, "Nonaqueous Sol – Gel Routes to Metal Oxide Nanoparticles," vol. 40, no. 9, pp. 793–800, 2007.

[81] T. J. Jacobsson, "Synthesis and characterisation of ZnO An experimental investigation of some of their size dependent quantum effects," *Mater. Chem.*, pp. 1–73, 2009.

[82] L. Znaidi, "Sol-gel-deposited ZnO thin films: A review," in *Materials Science and Engineering B: Solid-State Materials for Advanced Technology*, 2010, vol. 174, no. 1–

3, pp. 18–30.

[83] J. G. Mainz, “Preparation and Characterization of ZnO Nanoparticles by a Novel Sol – Gel Route Preparation and characterization of ZnO nanoparticles by a novel sol – gel route,” no. MARCH, pp. 2–6, 2007.

[84] M. Risti, “Sol-Gel Synthesis and Characterization of Nanocrystalline ZnO Powders,” no. March, 2016.

[85] S. S. Spin-coating, “Optical and Electrical Properties of (002) -Oriented ZnO Films Prepared on Amorphous,” vol. 19, no. 002, pp. 113–117, 2016.

[86] A. E. Morales, “Use of diffuse reflectance spectroscopy for optical characterization of un-supported nanostructures,” 2007.

[87] A. Al-kahlout, “Thermal treatment optimization of ZnO nanoparticles-photoelectrodes for high photovoltaic performance of dye-sensitized solar cells,” *J. Assoc. Arab Univ. Basic Appl. Sci.*, vol. 17, pp. 66–72, 2015.

[88] C. Lu and C. Yeh, “In ¯ uence of hydrothermal conditions on the morphology and particle size of zinc oxide powder,” vol. 26, pp. 351–357, 2000.

[89] D. Ramimoghadam, M. Zobir, B. Hussein, and Y. H. Taufiq-yap, “Hydrothermal synthesis of zinc oxide nanoparticles using rice as soft biotemplate,” pp. 1–10, 2013.

[90] A. R. Reddy, A. N. Mallika, K. S. Babu, and K. V. Reddy, “Hydrothermal Synthesis and Characterization of Zno Nano Crystals,” vol. 3, no. 2, pp. 2–5, 2015.

[91] D. Geetha and T. Thilagavathi, “HYDROTHERMAL SYNTHESIS OF NANO ZnO STRUCTURES FROM CTAB,” vol. 5, no. 1, pp. 297–301, 2010.

[92] P. M. Aneesh, K. A. Vanaja, and M. K. Jayaraj, “Synthesis of ZnO nanoparticles by

hydrothermal method," vol. 6639, no. 2007, pp. 1–9.

[93] S. Zhu, L. Shan, X. Tian, X. Zheng, D. Sun, and X. Liu, "Hydrothermal synthesis of oriented ZnO nanorod – nanosheets hierarchical architecture on zinc foil as fl exible photoanodes for dye-sensitized solar cells," *Ceram. Int.*, vol. 40, no. 8, pp. 11663–11670, 2014.

[94] D. Ahmed, M. Osman, and M. A. Mustafa, "Synthesis and Characterization of Zinc Oxide Nanoparticles using Zinc Acetate Dihydrate and Sodium Hydroxide," vol. 1, no. 4, pp. 248–251, 2015.

[95] A. Bagabas, A. Alshammari, M. F. A. Aboud, and H. Kosslick, "Room-temperature synthesis of zinc oxide nanoparticles in different media and their application in cyanide photodegradation," pp. 1–10, 2013.

[96] V. Fang, J. Futter, J. Kennedy, and J. Manning, "A review of near infrared reflectance properties of metal oxide nanostructures," no. July, 2013.

[97] K. Basu *et al.*, "Enhanced photovoltaic properties in dye sensitized solar cells by surface treatment of SnO2 photoanodes," *Sci. Rep.*, vol. 6, no. March, pp. 1–10, 2016.